LOCALIZED APPROXIMATION OF TIME DEPENDENT PARTIAL DIFFERENTIAL EQUATIONS USING RADIAL KERNELS

By

Kamran

Supervised by

Dr. Marjan Uddin

This thesis is submitted in partial fulfillment
of the requirements for the Degree of
Doctor of Philosophy

Department of Basic Sciences and Islamiat
University of Engineering and Technology, Peshawar
Pakistan
February 2018

To my parents and my children.

Table of Contents

List of Tables

List of Figures

Abstract

Time dependent partial differential equations (PDEs) model systems that experience change as a function of time. Time dependent PDEs have numerous applications such as diffusion, heat transfer, thermodynamics, population dynamics and wave phenomena. They are naturally parabolic or hyperbolic. Meshless methods have large advantages in accuracy over other methods, such as finite difference method (FDM), finite volume method (FVM), finite element method (FEM). The main features of the meshless methods are its simplicity, efficiency and invariance under euclidian transformation and can handle problems defined on complex shape domains. Meshless methods have some serious drawbacks as well. When the nodes are increased the method solve comparatively large system, and the ill-conditioning of the system matrix causes instability. Due to which it becomes difficult to achieve spectral convergence.

This thesis is concerned with two issues that is to solve the ill- conditioning problem of the interpolation matrix by radial kernels in local setting and to replace the time marching scheme with the numerical inversion of Laplace transforms which eliminates temporal truncation errors and the need for many time integration steps. The method is applied to solve fractional and integer order time dependent PDEs. The method comprises of three steps. First the Laplace transform is applied to the partial differential equation and boundary conditions in a given differential system. Second, the kernel based method is employed to solve the transformed differential system. Third, the solution is represented as a contour integral evaluated to high accuracy by trapezoidal rule.

Acknowledgements

My first thanks and heartfelt gratitude to Allah Almighty who encouraged this project and who steered me away from innumerable quick sands while it was merely a glimmer.

Next I cordially thank my supervisor Dr. Marjan Uddin for his kind supervision and valuable suggestions. Without his dynamic and motivational supervision, I would not have accomplished my project.

I would like to acknowledge all the support, useful discussions and countless debates with Prof Dr. Amjad Ali (Ex Chairman).

I am grateful to Research Evaluation Committee (REC) members Dr. Saeed Gul at UET Peshawar, Prof Dr. Sirajul Haq at GIKI and Dr. Suhail Khan at University of Peshawar for their advice and valuable ideas in completing this project.

Special thanks to vice chancellor Prof Dr. Iftikhar Hussain and Dean Prof Dr. Noor Muhammad for providing excellent research environment.

I am thankful to my graduate teachers Prof Dr. Siraj ul Islam(Chairman), Prof Dr. Ali Muhammad, Dr. Noor Badshah and Dr. Rehan Ali Shah for their support throughout my study. I would also like to thank my colleagues and friends Nadeem Jan and Aftab Alam, too many to mention, for their support and for providing me materials whenever I needed them. My acknowledgements, of course, will be incomplete without referring to my parents who always prayed for my success. I owe them more than I can duly acknowledge here. And finally, last but not the least, my special thanks to my wife who always supported and facilitated me in whatever capacity it was possible for her in my current endeavor.

February 2018 Kamran

Chapter 1

Introduction

1.1 Introduction

Time-dependent partial differential equations (PDEs) of integer and fractional order have applications in sciences and engineering such as heat transfer [1, 2], solute transport [3], long water waves [4], conservation laws[5], diffusion[6, 7], optoelectronic devices [8], Darcy flow [9], seepage [10], magnetic plasma [11], and electron transportation [12], etc. In finance such as tick-by-tick dynamics [13], American and European options[14, 15], American options[16, 17], European options[18, 19, 20], barrier options[21], etc. In biology such as tumor-induced angiogenesis[22], corneal epithelium [23], angiogenesis [24], genetic regulatory systems[25], wound healing assay[26, 27], other related models can be found in the books by Edelstein [28], and Murray [29, 30]. Many phenomena such as, mechanical properties of meterials [31, 32], mathematical models in finance[13, 33], signal processing [34], viscoelasticity and viscoplasticity [35, 36], and other can be successfully described by models from fractional calculus. Some of the most applications are given in the book of Podlubny [37], the book of Spanier and Oldham [38], and the papers of Bagley and Trovik [39], Metzler

and Klafter [40]. The analytical solution of these equations particularly in complex shaped and nonlinear cases is not easy to obtain. For the solution of such type of equations a large number of numerical methods are available such as, the finite difference method (FDM) [41], the finite element method (FEM) [42], the finite volume method (FVM) [43], the boundary element method (BEM)[44], etc. The mentioned methods are local mesh based interpolation methods. All these methods have powerful features, but there are some serious difficulties in applying them to geometrically complex three dimensional transient situations. For all these mentioned methods the need to create a polygonisation, either on its boundary or in the domain is the common drawback. Creating mesh is the most time consuming part of the solution process and for irregular geometry problems can occur with implementation. On contrary, meshless methods use a set of random or uniform points which are not connected in the form of a mesh. Meshless methods have the capability of interpolation with high accuracy and efficiency both locally and globally [45, 46, 47].

In recent years, some applications of meshless methods for integral and fractional order time dependent PDEs have been appeared such as, the moving least squares method for fractional advection diffusion equations [48], the meshless local Petrov-Galerkin method for 2D fractional convection diffusion reaction equations[49], the direct meshless local Petrov-Galerkin for fractional advection diffusion [50], the Kansa method for fractional diffusion equation [51], the local point interpolation method for $4th$ order initial boundary value problems for static and dynamic analysis of beams [52]. Some other meshless methods include the boundary particle method [53, 54], the boundary knot method [55, 56], the singular boundary method [57, 58], the regularized meshless method [59], the element free Galerkin methods [60], the diffuse element

method [61], RBF-MFS method [62], the method of approximate particular solutions (MAPS) [63], and the localized method of approximate particular solutions (LMAPS) [64], etc.

Comparatively, RBFs methods have the advantage that they do not require descretization and integration of domain or boundary. Since RBFs depends only on the distances between points, they can handle multi dimensional problems defined on complex domains.

The RBFs method is the generalized version of multiquadrics (MQ) method developed by Hardy [65] in 1971 for the approximation of 2D geographical surfaces based on scattered data. In 1975 thin-plate splines (TPS) was proposed by Duchon [66]. Until 1979 Hardy's interpolation scheme was unnoticed, then Richard Franke in his Papers [67, 68] compared different methods for the solution of scattered data interpolation. Frank concluded that Hardy's (MQ) scheme was the best. He also guessed that the method was well posed and the system matrix was invertible. In 1986 Charles Michilli proved that the system matrix of the (MQ) method was invertible[69]. In [70, 71] for the first time Kansa used (MQ) method for the solution of (PDEs) and this idea was extended in [72] afterwards, which is known as Kansa's method. In 1980s before Kansa's work Brebbia and Nardini [73] applied the function $1 + r$ an ad hoc RBF, as the basis function in the dual reciprocity method (DRM). This original work gave rise to currently popular dual reciprocity BEM (DR-BEM).

A large amount of work has been done related to accuracy and convergence of RBFs interpolation's [74, 75, 76, 77, 78, 79]. Madych and Nelson [80, 81, 82], Duchon [9], Cheng [83] and Schaback and Wu [84] estimated the error of RBFs interpolation. Wendland [85] summarized these estimates for various RBFs with respect to grid

size h. Buhmann [86, 87] proved (MQ) converges spectrally and faster as the spatial dimension increases. In [88] Schaback proved convergence of variations of the unsymmetric kernel-based collocation method introduced by Kansa in 1986.

Due to the early work by Kansa [89], Kansa and Moridis[90], Golberg [91], Dubal [92, 93], Kansa method become very popular and RBFs are affectively used to solve PDEs [94]. Using RBFs the numerical solutions of PDEs were theoretically proved by Franke and Schaback [95, 96]. Problems involving moving boundaries and large deformations are affectively handled with meshfree methods [97, 98]. For the solution of PDEs a symmetric and non-symmetric methods were suggested by Kansa [71], and Fasshauer [99] respectively. These methods are both originally used with globally supported basis functions. The issue of stability and numerical efficiency in these methods was addressed by Ling and Kansa [100, 101]. All these method are global radial basis functions collocation methods. These methods have numerous applications in engineering and sciences such as shallow water equations [102], European options [103], multi-asset American options [16], Stokes laws [104], groundwater contaminant transport [105], multi scale solidification modeling [106], diffusion [107], and others [108, 109, 110, 45, 111], etc.

Globally defined RBFs, generally results in a dense system matrix. Due to the ill-conditioning of the system matrix, solving large scale problem using RBFs faces difficulties. To handle this issue Wendland [112] and Wu [113] proposed a new type of RBFs defined as compactly-supported positive definite RBFs (CS-RBFs) to make the system matrix sparse. Fasshauer [114] discussed the differences between globally and locally supported methods, also an important role of smoothing within a multilevel framework is demonstrated for locally supported methods. He has explored

a possible connection between multigrid finite elements and multilevel radial basis function methods with smoothing. Zhou et al.[115] have incorporated overlapping domain decomposition technique to overcome the problem of ill-conditioning. Kansa and Hon [116] also used the domain decomposition techniques. Hon used the greedy algorithm technique [117] to circumvent the issue of ill-conditioning. To affectively handle these issues another way is to use the recently developed local radial basis functions method.

Local radial basis functions collocation method was introduced in [118] to circumvent the problem of ill-conditioning and shape parameter sensitivity of the global radial basis functions method. A clear improvement is observed in terms of accuracy and efficiency. Due to the efficiency of local radial basis functions method researchers applied it to more complex and large scale problems such as Navier-Stokes equations [119], solid-liquid phase change problems [120], aluminum billet casting [121], phase-field problems [122], computational fluid dynamics [123], heat transfer and fluid flow [124], Darcy flow [9], turbulent flow [125], diffusion Equation [126], wave equations [127], fractional diffusion equations [128], thermo-driven fluid-flow [129], and convection dominated problems [130], etc. These methods use finite differnce time stepping procedure. The drawback of time stepping techniques is the possibility of stability restrictions. To avoid temporal discretization and time instability Laplace transform is used.

The Laplace transform was first used by Rizzo and Shippey [131] parallel with the boundary integral equation method, in which the authors used Prony series [132, 133] for inversion. The fourier series was used by the author's in [134] for the numerical

inversion of Laplace transform, and this method was improved in [135]. Other numerical methods [136, 137, 138] were proposed to speed up the convergence of the methods [134, 135]. In [139, 140, 141] the author's used stehfest method [142, 143] for numerically inverting the solutions of radial transport in Laplace space. The Crump technique [138] was introduced in[144, 145, 146, 147] for the Laplace transform inversion. This method utilizes the epsilon algorithm for calculating the complex Fourier series real part when handling the integral of the inverse Laplace transform. For computing the full Fourier series, De Hoog et al. [148] used the epsilon or quotient difference algorithm. Using this technique the Crump method [138] has been improved and the convergence of the series is accelerated. The method proposed in [148] has many applications such as to invert the Laplace transform for radial dispersion [149, 150]. Moench [151] used the Talbot method [152], he pointed out that the method may not be stable while inverting a function with a steep front. Some work has been done in [153] for generalizing the Talbot's method. The author's [154, 155] approximated the inverse Laplace transform by employing the Stehfest method [142, 143]. Numerous methods were used by different researchers for numerically inverting the Laplace transform such as the Crump method [138] was used by the author's [156, 157], the Weeks [158] method by [159], and the De Hoog method [148] by [156, 160, 161]. Except these methods, so many other methods[162, 163, 164, 165, 166, 167, 168, 136, 169] were developed for numerically inverting the Laplace transform. The Laplace transform finite difference method were used for simulation of flow through porous media [170], compressible liquid flow in reservoirs [171] and the numerical inversion of Laplace transform was done using Stehfest method [142]. In [172] the author's used Laplace transform finite element method for the solution ground water equation. The Laplace

transform boundary element method was used for solution of diffusion type equations [173] and diffusion problems [174]. In [90] the authors have combined the Laplace transform with multi quadric method and for inversion the Stehfest [142], and De Hoog [148] methods were used. Similarly the author's combined the Laplace transform with galerkin method [175], boundary particle method [176], and RBFs method on unit sphere [177]. Recently some of the most efficient methods for approximating the inverse Laplace transform depending on the approximation of Bromwich contour integral are proposed. The author's in [178, 179, 180, 181] coupled the Laplace transform with finite element method. The spectral method is combined with Laplace transform in [182, 183, 184, 185]. The accuracy of these methods depend on the optimal contour of integration.

In this dissertation we have combined the Laplace transform with local kernel based method to overcome the problem of severe ill conditioning of the system matrix and to avoid temporal discretization, because of the temporal discretization these methods encounter an exponential increase of computing costs with advancing time and thus have low efficiency in the simulation. In order to overcome this drawback the Laplace transformation is used to avoid the time stepping.

In Laplace transform based method the Laplace transform is applied to the given time dependent problem and the resulting time independent problem is solved in Laplace space with local radial basis functions method and the solution is then inverted using inverse Laplace transform. However, the analytical inversion is too difficult, alternatively the numerical inversion is performed using the Browmwich integral approximation by trapezoidal rule.

1.2 Overview of the thesis

In next section some preliminaries related to radial kernels and Laplace transform are discussed.

In chapter 2, Laplace transform local kernel based method is described for approximating time dependent PDEs of order α, where $p-1 \leq \alpha \leq p,\ p \in \mathbb{N}$, with some given initial and boundary conditions. The stability and convergence of the proposed method is discussed.

In chapter 3, the Laplace transform local kernel based method is applied to integer and fractional order diffusion equations and the results are compared with the existing time stepping methods for the given problems.

In chapetr 4, the Laplace transform local kernel based method is tested for fractional diffusion wave equation.

In chapter 5, the method is applied to fractional telegraph equations.

In chapter 6, the method is tested for partial integro differential equation.

1.3 Preliminaries

This section is devoted to basic definitions and results related to radial kernels and Laplace transform. The details can be found in the books [45, 186, 38]

Definition 1.3.1. A kernel K is nothing but a real-valued function of two variables, i.e.,

$$K : \Omega \times \Omega \to \mathbb{R}, \tag{1.3.1}$$

Here Ω is usually a subset of $\mathbb{R}^d$.

Definition 1.3.2. A function $\Phi : \mathbb{R}^d \longrightarrow \mathbb{R}$ is called radial if there exists a univariate function $\phi : [0, \infty) \longrightarrow \mathbb{R}$ such that

$$\Phi(x) = \phi(r),$$

where $r = \|x\|$, and $\|.\|$ is a norm on $\mathbb{R}^d$($\|.\|$ is typically the Euclidean norm.)

Categories of radial kernels(RBFs)

There are three categories of radial basis functions, compactly supported, globally supported finitely differentiable, and globally supported infinitely differentiable radial basis functions.

1. **Compactly supported RBFs:** Compactly supported RBFs achieve algebraic convergence rate, some compactly supported RBFs are:

Dimension	RBFs	$\phi(r)$	Continuity of function
$d=1$	$\phi_{1,0}$	$(1-\varepsilon r)_+$	C^0
	$\phi_{1,1}$	$(1-\varepsilon r)_+^3(1+3\varepsilon r)$	C^2
	$\phi_{1,2}$	$(1-\varepsilon r)_+^5(1+5\varepsilon r+8\varepsilon^2 r^2)$	C^4
$d=3$	$\phi_{3,0}$	$(1-\varepsilon r)_+^2$	C^0
	$\phi_{3,1}$	$(1-\varepsilon r)_+^4(1+4\varepsilon r)$	C^2
	$\phi_{3,2}$	$(1-\varepsilon r)_+^6(3+18\varepsilon r+35(\varepsilon r)^2)$	C^4
	$\phi_{3,3}$	$(1-\varepsilon r)_+^8(1+8\varepsilon r+25(\varepsilon r)^2+32(\varepsilon r)^3)$	C^6
$d=5$	$\phi_{5,0}$	$(1-\varepsilon r)_+^3$	C^0
	$\phi_{5,1}$	$(1-\varepsilon r)_+^5(5\varepsilon r+1)$	C^2
	$\phi_{5,2}$	$(1-\varepsilon r)_+^7(16\varepsilon^2 r^2+7\varepsilon r+1)$	C^4

Table 1.1: Wendland's CR-RBFs

2. **Globally supported finitely differentiable RBFs:** Globally supported finitely differentiable RBFs also have algebraic convergence rates. Globally supported finitely differentiable RBFs are:

RBFs	$\phi(r)$
Power kernels	r^{2m-1}, $m \in \mathbb{N}$
Polyhormonic	r^{2m}log(r), $m \in \mathbb{N}$
Thin-plate spline	r^2log(r)

3. **Globally supported infinitely differentiable RBFs:** Globally supported infinitely differentiable RBFs have spectral convergence rate:

RBFs	$\phi(r)$
Guassian	$e^{-\varepsilon^2 r^2}$
Multiquadrics	$(1+\varepsilon^2 r^2)^m,\ m>0, m\notin\mathbb{N}$
Inverse multiquadric	$(1+\varepsilon^2 r^2)^{-m},\ m>0, m\notin\mathbb{N}$

Definition 1.3.3. When the error decays at the rate $O(N^{-m}),\ m\in\mathbb{R}$, then algebraic convergence rates occur.

Definition 1.3.4. When the error decays at the rate $O(\eta^N),$ for increasing $N,$ where $0<\eta<1$, then spectral convergence rates occur.

Definition 1.3.5. The Laplace transform of a function $u(t)$ is defined as

$$\mathscr{L}\{u(t)\}=\hat{u}(z)=\int_0^\infty e^{-zt}u(t)dt,\ Re(z)>0. \tag{1.3.2}$$

Definition 1.3.6. Assume the function $u(t)$ is continuous over $0\le t\le T$, if there exist constants γ and μ such that,

$$\mid e^{-\mu t}u(t)\mid<\gamma,\forall\ t>T, \tag{1.3.3}$$

then the Laplace transform of $u(t)$ exists.

Definition 1.3.7. The inverse Laplace transform is defined as

$$\mathscr{L}^{-1}\{\hat{u}(z)\}=u(t)=\frac{1}{2\pi\iota}\int_{\sigma-\iota\infty}^{\sigma+\iota\infty}e^{zt}\hat{u}(z)dz,\ \sigma>0. \tag{1.3.4}$$

Theorem 1.3.1. *(Convolution Theorem) If* $\mathscr{L}\{f(t)\}=F(z)$ *and* $\mathscr{L}\{g(t)\}=G(z)$, *then* $\mathscr{L}\{f(t)*g(t)\}=\mathscr{L}\{f(t)\}\mathscr{L}\{g(t)\}=F(z)G(z)$,

where $f(t) * g(t)$ is the convolution of $f(t)$ and $g(t)$ defined by,

$$f(t) * g(t) = \int_0^t f(t-s)g(s)ds.$$

Definition 1.3.8. The Riemann-Liouville, integral of order $\alpha \in \mathbb{R}^+$ of a function $u(t)$ is defined as (see [38])

$$D_t^{-\alpha}u(t) = \frac{1}{\Gamma(\alpha)}\int_0^t (t-s)^{\alpha-1}u(s)ds \tag{1.3.5}$$

Definition 1.3.9. The Riemann-Liouville derivative of fractional order α of a function $u(t)$ is defined as (see [38])

$${}_{RL}D_t^{-\alpha}u(t) = \frac{1}{\Gamma(p-\alpha)}\frac{d^p}{dt^p}\int_0^t (t-s)^{p-\alpha-1}u(s)ds, \tag{1.3.6}$$

where, $p-1 \leq \alpha \leq p,\ p \in \mathbb{N}$.

Definition 1.3.10. The Caputo fractional partial derivative of order α of a function $u(t)$ is defined by(see [38]).

$${}_{C}D_t^{-\alpha}u(t) = \frac{1}{\Gamma(p-\alpha)}\int_0^t (t-s)^{p-\alpha-1}\frac{d^p}{ds^p}u(s)ds, \tag{1.3.7}$$

$p-1 \leq \alpha \leq p,\ p \in \mathbb{N}$.

Property 1.3.2. *If $u(t) \in C^p[0,\infty)$ and $p-1 < \alpha < p,\ p \in \mathbb{N}$, then,*

$${}_{C}D_t^{-\alpha}u(t) = {}_{RL}D_t^{-\alpha}u(t)\left(u(t) - \sum_{i=0}^{p-1}\frac{t^i}{i!}u^{(i)}(0)\right). \tag{1.3.8}$$

Property 1.3.3. *If $u(t) \in C^p[0,\infty)$ and $p-1 < \alpha < p,\ p \in \mathbb{N}$, then, the Laplace transform of the Caputo fractional derivative is given by*

$$\mathscr{L}\{{}_{C}D_t^{-\alpha}u(t)\} = z^{\alpha}\hat{u} - \sum_{i=0}^{p-1} z^{\alpha-i-1}u^{(i)}(0). \tag{1.3.9}$$

Definition 1.3.11. The Mittag-liffler function is denoted by $E_\alpha(z)$ and is defined as

$$E_\alpha(z) = \sum_{m=0}^{\infty} \frac{z^m}{\Gamma(1+\alpha m)},\ \mathcal{R}(\alpha) > 0. \tag{1.3.10}$$

In literature a large number of contour's have been devised for numerical inversion of Laplace transform. Some of them are defined as follows:

1. **Talbot's contour:** The Talbot's contour is defined as [187]

$$z(\theta) = \sigma + \lambda z_\nu(\theta),\ \theta \in (-2\pi\iota, 2\pi\iota), \tag{1.3.11}$$

where,

$$z_\nu(\theta) = \frac{\theta}{1-e^{-\theta}} + \theta\frac{\nu-1}{2},$$

using $\theta = 2\iota\varrho$ in (1.3.11), the contour is parameterized as

$$z(\varrho) = \sigma + \lambda z_\nu(\varrho),\ \varrho \in (-\pi, \pi), \tag{1.3.12}$$

where,

$$z_\nu(\varrho) = \varrho\cot\varrho + \iota\nu\varrho,$$

the real parameters $\lambda > 0$, $\nu > 0$, σ determines the curve's geometry.

2. **Modified Talbot's contour:** The modified form of Talbot's contour is [188]

$$\begin{aligned} &z(\varrho) = \frac{M}{t}\xi(\varrho), \\ &\xi(\varrho) = -\sigma + \lambda\varrho\cot(\alpha\varrho) + \nu\iota\varrho,\ \ -\pi \le \varrho \le \pi, \\ &M \longrightarrow \infty,\ t \text{ fixed}, \end{aligned} \tag{1.3.13}$$

here $\sigma, \lambda, \nu, \alpha$ are constants to be specified by the user.

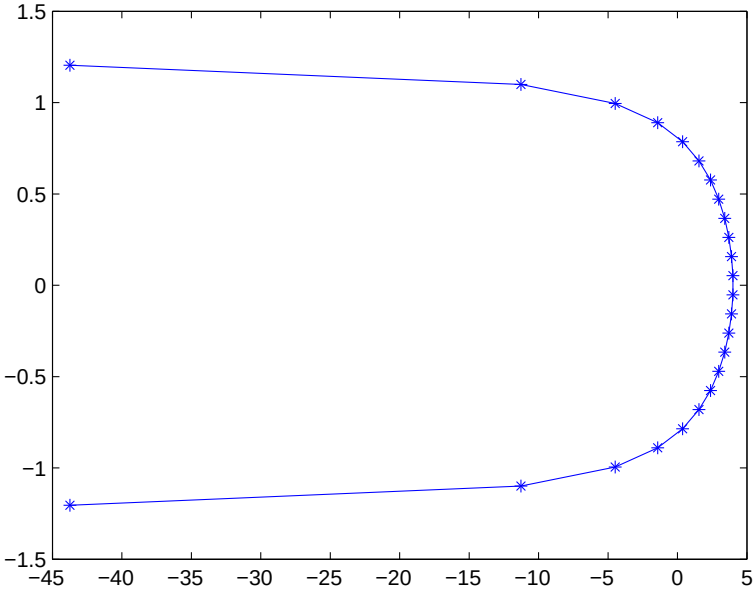

Figure 1.1: Talbot's Contour

3. **Parabolic contour:**[185] The parabolic contour in parametric form is given by

$$z = \xi(\iota\varrho + 1)^2, \tag{1.3.14}$$

For the strip $\varrho = \zeta + \iota c$, where $c > 0$, $-\infty < \zeta < \infty$, the parabolic contour reduces to

$$z(\zeta) = \xi\left((1-c)^2 - \zeta^2\right) + 2\iota\xi\zeta(1-c), \qquad (C_1) \tag{1.3.15}$$

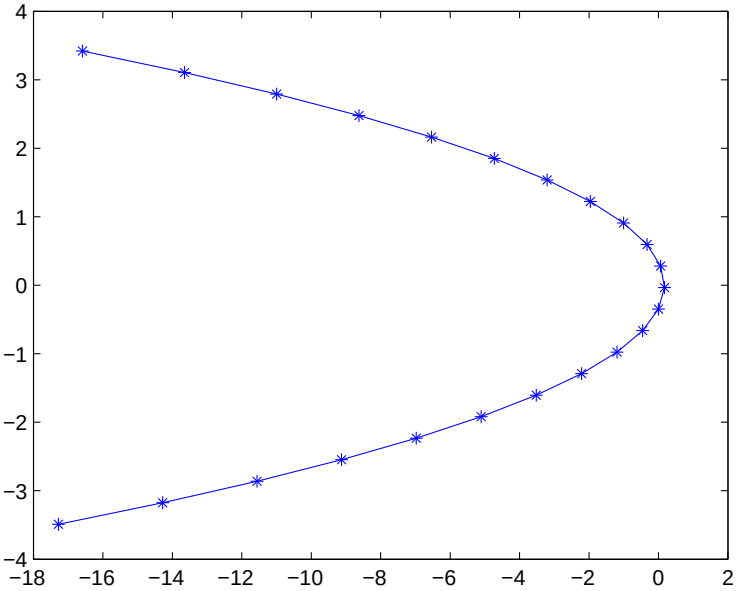

Figure 1.2: Parabolic Contour

4. **Hyperbolic contour:**[185] The hyperbolic contour in parametric form is given by

$$z = \xi(1 + \sin(i\varrho - \alpha)), \quad -\infty < \varrho < \infty, \tag{1.3.16}$$

For the strip $\varrho = \zeta + \iota c$, where $c > 0$, $-\infty < \zeta < \infty$, the hyperbolic contour reduces to

$$z(\zeta) = \xi\,(1 - \sin(\alpha + c)\cosh(\zeta)) + \iota\xi\cos(\alpha + c)\sinh(\zeta). \qquad (C_2) \tag{1.3.17}$$

where the contour width is controlled by the parameter ξ and the parameter α determines the asymptotic angle.

5. **Modified hyperbolic contour:**[181] Another form of the hyperbolic contour used in our computation is given in parametric form as

$$z(\zeta) = \omega + \lambda\left(1 - sin(\delta - \iota\zeta)\right), for\ \zeta \in \mathbb{R}, \quad (C_3) \tag{1.3.18}$$

with $\lambda > 0$, $\omega \geq 0$, $0 < \delta < \beta - \frac{1}{2}\pi$, and $\frac{1}{2}\pi < \beta < \pi$, when $Im\zeta = \eta$, then (1.3.18) reduces to the left branch of hyperbola

$$\left(\frac{x - \omega - \lambda}{\lambda \sin(\delta + \eta)}\right)^2 - \left(\frac{y}{\lambda \cos(\delta + \eta)}\right)^2 = 1, \tag{1.3.19}$$

the strip $Y_r = \{\zeta : Im\zeta \leq r\}$, with $r \geq 0$ is transformed onto the hyperbola $\Omega_r = \{z : \xi \in Y_r\} \supset C_3$. Let $\Sigma_\varphi = \{z \neq 0 : |argz| \leq \varphi\} \cup \{0\}$, with $0 < \varphi < \frac{(1-\alpha)\pi}{2}$, and let $\Sigma_\beta^\omega = \lambda + \Sigma_\beta, C_3 \subset \Omega_r \subset \Sigma_\beta^\omega$.

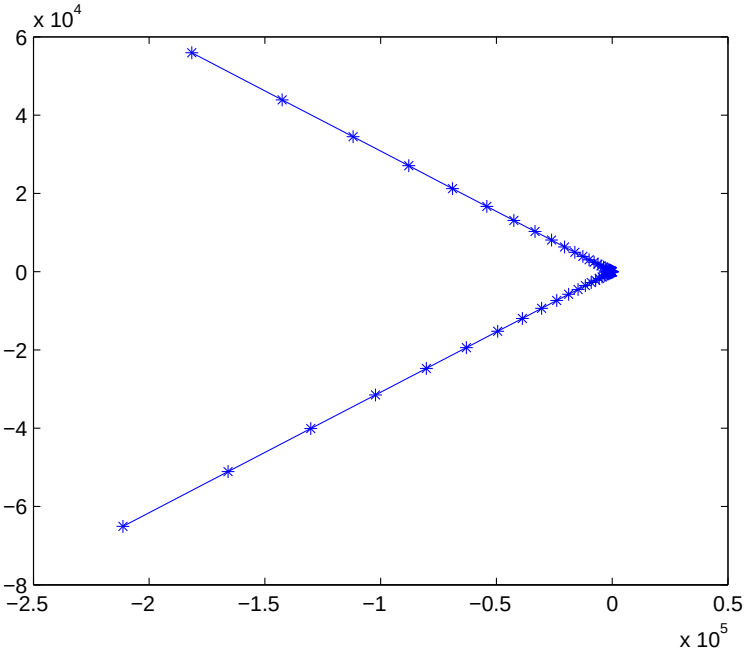

Figure 1.3: Hyperbolic Contour

1.4 Chapter summary

In this chapter some basic definitions related to Laplace transform and radial kernels are discussed. Three types of contours Talbot's contour, parabolic contour and hyperbolic contour are defined and their plots are given, which are used in our computations. In next chapter we describe the Laplace transform local kernel based method in some detail.

Chapter 2

Laplace transform local kernel based method

2.1 Introduction

Recently fractional calculus have gained popularity, and many researchers are attracted towards this field [189, 190, 37, 191, 192, 193, 194]. The theoretical analysis have been carried on in [195, 196]. Most of fractional differential equations can not be solved analytically, so the researchers have used numerical solution strategies based on stability and convergence analysis [197, 198, 199, 200, 201, 202]. In literature so many other works for approximation of fractional order PDEs can be found such as Adomian decomposition method [203], variational iteration method [204, 205], finite difference method [193, 206, 200, 207, 208], homotopy analysis method [209, 210], Pseudo-spectral method [201], finite element method [211, 212], RBFs method [213, 51, 214, 215], etc.

In this chapter we describe our method based on local radial kernels and Laplace transform for the solution of integral and fractional order time dependent partial differential equations. We consider a time fractional partial differential equation of

the form

$$\begin{aligned} &\partial_t^\alpha u(\mathbf{x},t) + \mathcal{L}u(\mathbf{x},t) = r(\mathbf{x},t),\ p-1 \le \alpha \le p,\ p \in \mathbb{N}, \\ &\mathbf{x} \in \Omega \subset \mathbb{R}^d,\ d \ge 1,\ t \in (t_0, T). \end{aligned} \tag{2.1.1}$$

with the initial conditions

$$u^i(\mathbf{x},0) = u^i(\mathbf{x}),\ i = 0,1,...,p-1,\ \mathbf{x} \in \Omega, \tag{2.1.2}$$

and the boundary conditions

$$\mathcal{B}u(\mathbf{x},t) = g(\mathbf{x},t),\ \mathbf{x} \in \partial\Omega,\ t \in (t_0, T). \tag{2.1.3}$$

where $\mathcal{L}$ is a linear spatial differential operator and $\mathcal{B}$ is boundary operator and ∂_t^α is the Caputo fractional partial derivative of order α. Then applying the Laplace transform to equation (2.1.1)-(2.1.3), we get

$$z^\alpha \hat{u}(\mathbf{x},z) - \sum_{i=0}^{p-1} z^{\alpha-i-1} u^{(i)}(\mathbf{x}) + \mathcal{L}\hat{u}(\mathbf{x},z) = \hat{r}(\mathbf{x},z),\ \mathbf{x} \in \Omega, \tag{2.1.4}$$

and

$$\mathcal{B}\hat{u}(\mathbf{x},z) = \hat{g}(\mathbf{x},z),\ \mathbf{x} \in \partial\Omega, \tag{2.1.5}$$

respectively. Where $\hat{r}(\mathbf{x},z)$ and $\hat{g}(\mathbf{x},z)$ are the corresponding Laplace transforms of $r(\mathbf{x},t)$ and $g(\mathbf{x},t)$ respectively. Thus we have the following system of linear differential equations

$$\left(z^\alpha I + \mathcal{L}\right)\hat{u}(\mathbf{x},z) = F(\mathbf{x},z),\ \mathbf{x} \in \Omega, \tag{2.1.6}$$

$$\mathcal{B}\hat{u}(\mathbf{x},z) = \hat{g}(\mathbf{x},z),\ \mathbf{x} \in \partial\Omega, \tag{2.1.7}$$

where,

$$F(\mathbf{x},z) = \sum_{i=0}^{p-1} z^{\alpha-i-1} u^{(i)}(\mathbf{x}) + \hat{r}(\mathbf{x},z).$$

The Laplace transform method evades costly convolution integral calculation of time fractional derivative and avoids the effect of time step on numerical accuracy and stability in comparison with finite difference discretization. In the next section the kernel based method in local setting is employed to solve the time independent problem (2.1.6)-(2.1.7) in Laplace space.

2.2 Local kernel based method

The system (2.1.6)-(2.1.7) contain the governing differential operator $\mathcal{L}$ and the boundary differential operator $\mathcal{B}$. In this section the local radial basis function scheme is constructed to approximate these two operators and to solve the system in Laplace space. Let $\{\mathbf{x}_i\}_{i=1}^N \in \Omega \subset \mathbb{R}^d, d \geq 1$, approximation of the solution $\hat{u}(\mathbf{x})$ by local kernel based method is defined as

$$\hat{u}^i(\mathbf{x}_i) = \sum_{\mathbf{x}_h \in \Omega_i} \alpha_h^i \phi(\|\mathbf{x}_i - \mathbf{x}_h\|), \tag{2.2.1}$$

where $\boldsymbol{\alpha}^i = [\alpha_1^i, \alpha_2^i, ..., \alpha_n^i]^T$ is the vector of coefficients, $\Omega_i \subset \Omega$ is a local domain which contains $\mathbf{x}_i$ and its n neighboring centers, and $\psi(r)$, $r \geq 0$ is a radial kernel. From (2.2.1), we get N number of linear systems of order $n \times n$ as follows

$$\hat{\mathbf{u}}^i = \Phi^i \boldsymbol{\alpha}^i, \ i = 1, 2, ..., N, \tag{2.2.2}$$

the entries of Φ^i are $b_{lh}^i = \phi(\|\mathbf{x}_l - \mathbf{x}_h\|), \ \mathbf{x}_l, \mathbf{x}_h \in \Omega_i$, the matrix Φ^i is called the interpolation matrix. It can be proved that the interpolation matrix is invertible if $\phi(r)$ is positive definite and the nodes are distinct. We need to solve each small linear system for the unknowns $\boldsymbol{\alpha}^i = [\alpha_1^i, \alpha_2^i, ..., \alpha_n^i]^T$. Similarly we approximate the operator $\mathcal{L}\hat{u}(\mathbf{x})$, by

$$\mathcal{L}\hat{u}^i(\mathbf{x}_i) = \sum_{\mathbf{x}_h \in \Omega_i} \alpha_h^i \mathcal{L}\phi(\|\mathbf{x}_i - \mathbf{x}_h\|), \tag{2.2.3}$$

writing (2.2.3) as a product of two vectors, given by

$$\mathcal{L}\hat{\mathbf{u}}^i = \mathbf{v}^i \cdot \boldsymbol{\alpha}^i, \tag{2.2.4}$$

where $\boldsymbol{\alpha}^i$ of order $n \times 1$ is a vector of unknown coefficients, and $\mathbf{v}^i$ is a vector with entries given by

$$\mathbf{v}^i = \mathcal{L}\phi(\|\mathbf{x}_i - \mathbf{x}_h\|),\ \mathbf{x}_h \in \Omega_i, \tag{2.2.5}$$

using equation (2.2.2), we eliminate the unknown coefficients,

$$\boldsymbol{\alpha}^i = (\Phi^i)^{-1}\hat{\mathbf{u}}^i, \tag{2.2.6}$$

by inserting the values of $\boldsymbol{\alpha}^i$ from (2.2.6) in (2.2.4) to get,

$$\mathcal{L}\hat{\mathbf{u}}^i = \mathbf{v}^i(\Phi^i)^{-1}\hat{\mathbf{u}}^i = \mathbf{w}^i\hat{\mathbf{u}}^i \tag{2.2.7}$$

where,

$$\mathbf{w}^i = \mathbf{v}^i(\Phi^i)^{-1}. \tag{2.2.8}$$

Hence for each center, the localized approximation of the linear differential operator using radial kernel functions is given by

$$\mathcal{L}\hat{\mathbf{u}} \equiv \boldsymbol{\Psi}\hat{\mathbf{u}}, \tag{2.2.9}$$

So the spatial operator $\mathcal{L}$ is approximated by the $N \times N$ sparse differentiation matrix $\boldsymbol{\Psi}$. Each row of $\boldsymbol{\Psi}$ have n non-zeros entries while $N - n$ zeros entries, where n is the number of nodes in the each local domain Ω_i. Similarly the boundary operator $\mathcal{B}$ can be approximated using the localized kernel based method discussed above.

2.2.1 Choosing optimal shape parameter

A variety of radial kernel functions are available in the literature. In this dissertation the multiquadrics (MQ) radial kernels defined by $\phi(r,\varepsilon) = \sqrt{1+(\varepsilon r)^2}$, the Inverse multiquadrics (IMQ) defined by $\phi(r,\varepsilon) = \frac{1}{\sqrt{1+(\varepsilon r)^2}}$, and the Gaussian radial kernel (Gus) defined by $\phi(r,\varepsilon) = e^{-\varepsilon^2 r^2}$ are chosen. Here the radial kernel functions contain the parameter ε which changes the shape of radial function. Variation of the kernel shape affects the accuracy of the solution. Better accuracy always needs optimal value of shape parameter. For choosing such optimal value of parameter a large amount of work is available in the literature for example some of such work can be found in [216, 217, 218, 219, 220, 221, 222], etc. In the work of [223] the uncertainty principle (e.g better accuracy can be achieved comparatively at larger condition numbers of these type of kernel based system matrices) related to the condition number of the system matrix is used for a nice estimation of the shape parameter ε.

Algorithm:

- Kept approximately the condition number in the range $10^{12} < \kappa < 10^{16}$ for our problem system matrices.

- Decompose the interpolation matrix as $[\mathbf{Q}, \mathbf{P}, \mathbf{V}] = svd(\Phi^i)$. Here SVD is the singular value decomposition of the interpolation matrix Φ^i of order $n \times n$ corresponding to each local sub-domain Ω_i, and $\mathbf{P}$ is the diagonal matrix having n singular values of Φ^i, and $\kappa = \|\Phi^i\|\|(\Phi^i)^{-1}\| = \max(\mathbf{P})/\min(\mathbf{P})$, denotes condition number of matrix Φ^i.

- Search for ε until κ satisfy the condition $10^{12} < \kappa < 10^{16}$, using the algorithm

  $\kappa = 1$

  $10^{12} < \kappa < 10^{16}$

  while $\kappa < \kappa_{min}$ and $\kappa > \kappa_{max}$

  $\mathbf{Q}, \mathbf{P}, \mathbf{V} = svd(\Phi^i)$

  $\kappa = \max(\mathbf{P})/\min(\mathbf{P})$

  if $\kappa < \kappa_{min},\ \varepsilon = \varepsilon - \delta\varepsilon$

  if $\kappa > \kappa_{max},\ \varepsilon = \varepsilon + \delta\varepsilon$

  ε (optimal) $= \varepsilon$.

  When the above condition is satisfied a good value of ε is obtained, the inverse is computed using, $(\Phi^i)^{-1} = (\mathbf{QPV^T})^{-1} = \mathbf{VP^{-1}Q^T}$. Thus we can compute $\mathbf{w}^i$ in (2.2.8).

2.3 Stability

To discuss the stability of system (2.1.6)-(2.1.7), in discrete form this system can be represented as

$$\mathbf{H\hat{u}} = \mathbf{b}, \tag{2.3.1}$$

where $\mathbf{H}$ is $N \times N$ sparse differentiation matrix which can be obtained by localized kernel based method as discussed. The stability constant [224] corresponding to system (2.3.1) is defined by

$$C = \sup_{\hat{\mathbf{u}} \neq 0} \frac{\|\hat{\mathbf{u}}\|}{\|\mathbf{H\hat{u}}\|}. \tag{2.3.2}$$

The value of C is finite using any type of discrete norms $\|.\|$ on $\mathbb{R}^N$. The above equation can be expressed as

$$\|\mathbf{H}\|^{-1} \leq \frac{\|\hat{\mathbf{u}}\|}{\|\mathbf{H}\hat{\mathbf{u}}\|} \leq C, \tag{2.3.3}$$

Again in terms of Pseudoinverse $\mathbf{H}^\dagger$ of $\mathbf{H}$, we have

$$\|\mathbf{H}^\dagger\| = \sup_{\mathbf{v}\neq 0} \frac{\|\mathbf{H}^\dagger \mathbf{v}\|}{\|\mathbf{v}\|}. \tag{2.3.4}$$

Now we write

$$\|\mathbf{H}^\dagger\| \geq \sup_{\mathbf{v}=\mathbf{H}\hat{\mathbf{u}}\neq 0} \frac{\|\mathbf{H}^\dagger \mathbf{H}\hat{\mathbf{u}}\|}{\|\mathbf{H}\hat{\mathbf{u}}\|} = \sup_{\hat{\mathbf{u}}\neq 0} \frac{\|\hat{\mathbf{u}}\|}{\|\mathbf{H}\hat{\mathbf{u}}\|} = C. \tag{2.3.5}$$

Hence equations (2.3.3) and (2.3.5) defines the bounds of the stability constant C. For numerical approximation of the system (2.3.1) calculation of Pseudoinverse may be computationally expansive, but it ensures numerical stability. In case of square systems, the MATLAB's function **condest** gives an estimate of L_∞ norm of $\mathbf{H}^{-1}$, thus we have

$$C = \frac{condest(\mathbf{H}')}{\|\mathbf{H}\|_\infty} \tag{2.3.6}$$

For our sparse differentiation matrix $\mathbf{H}$ this work well with less computations. The bounds of the stability constant C are shown in the Figure 2.1 corresponding to Problem 3.2.1. Choosing $M = 60$, $N = 35$ and $n = 10$ at time $t = 1$, we can see that $1 \leq C \leq 2.3097$ which show the stability constant is bounded by very small numbers, which imply the stability of our localized numerical scheme.

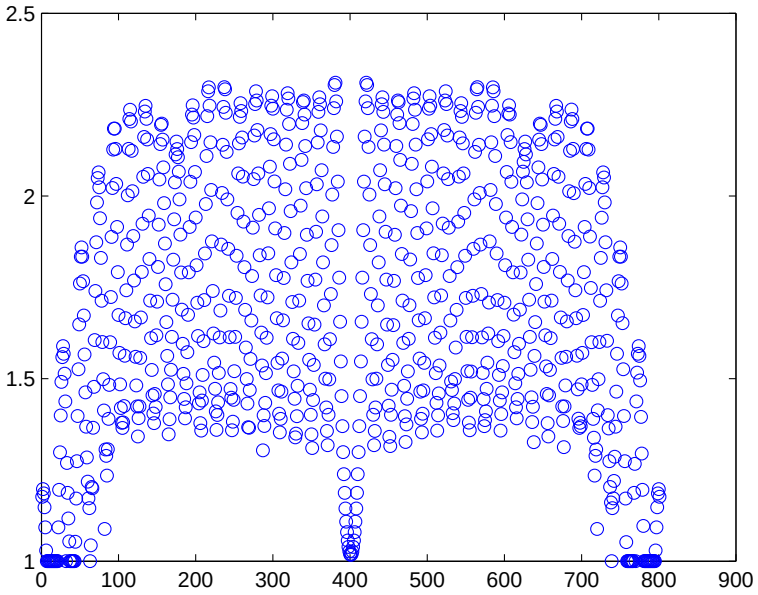

Figure 2.1: The plot of the stability constant C of our differentiation matrix $\mathbf{H}$ for different quadrature points along the parabolic contour C_1 corresponding to problem 3.2.1.

2.4 Numerical inversion of Laplace transform

In this section numerical inverse Laplace transform is implemented to obtain the solution of the problem defined by (2.1.1)-(2.1.3). Here we compute the inversion through contour integral representation of the form

$$u(\mathbf{x},t) = \frac{1}{2\pi i}\int_{\sigma-i\infty}^{\sigma+i\infty} e^{zt}\hat{u}(\mathbf{x},z)dz = \frac{1}{2\pi i}\int_{\Gamma} e^{zt}\hat{u}(\mathbf{x},z)dz, \quad \sigma > \sigma_0, \tag{2.4.1}$$

where Γ is the contour of integration connecting $\sigma - i\infty$ to $\sigma + i\infty$, defined by the equations (1.3.15), (1.3.17), or (1.3.18)

Using either of the parabolic or hyperbolic contour defined by (1.3.15), (1.3.17),

or (1.3.18) the integral representation (2.4.1), becomes

$$u(\mathbf{x},t)=\frac{1}{2\pi i}\int_{-\infty}^{\infty}e^{z(\zeta)t}\hat{u}(\mathbf{x},z(\zeta))\acute{z}(\zeta)d\zeta, \tag{2.4.2}$$

The approximation of (2.4.2) by trapezoidal rule with uniform step size k, and quadrature points $z_j=z(\zeta_j),\zeta_j=jk$, is given as

$$u_k(\mathbf{x},t)=\frac{k}{2\pi i}\sum_{j=-M}^{M}e^{z_jt}\hat{u}(\mathbf{x},z_j)\acute{z}_j. \tag{2.4.3}$$

Since in our computation we used trapezoidal rule, the error bounds for parabolic contour C_1 defined by (1.3.15) and hyperbolic contour C_2 defined by (1.3.17) are based on the following theorem.

Theorem 2.4.1. *[185] Let $z=x+\iota y,\ x,y\in\mathbb{R}$. Suppose $G(z)$ is analytic in the strip $-d<y<c$, for some $d>0,c>0$, with $G(z)\to 0$, as $|z|\to\infty$ in the strip. Suppose for constants W_+,W_- the function $G(z)$ satisfies*

$$\int_{-\infty}^{\infty}|G(x+\iota r)|dx\le W_+, \tag{2.4.4}$$

$$\int_{-\infty}^{\infty}|G(x-\iota s)|dx\le W_-, \tag{2.4.5}$$

$\forall\ 0<r<c,\ 0<s<d$. Then the error estimate is

$$|u_k(\mathbf{x},t)-u(\mathbf{x},t)|=\frac{2W}{e^{\frac{2\pi c}{k}}-1}$$

For best accuracy we need to find the optimal contour of integration. In the work [185] derive an efficient method for determining optimal contour of integration. They determine optimal values of the parameters μ, α and k by asymptotically balancing the truncation error and descretization errors in each of the half plans. The optimal parameters for parabolic contour defined by (1.3.15) for given t_0, t, T, and M are given by $\mu=\frac{\pi}{4\sqrt{8\Lambda+1}}\frac{M}{t}$, $k=\frac{\sqrt{8\Lambda+1}}{M}$, $\Lambda=\frac{T}{t_0}$. For these parameters the error estimate is of the order

$$E_1=|u_k(\mathbf{x},t)-u(\mathbf{x},t)|=O\left(e^{-\left(\frac{2\pi}{\sqrt{8\Lambda+1}}\right)M}\right),M\to\infty \tag{2.4.6}$$

The optimal values of parameters for hyperbolic contour defined by (1.3.17), proposed in [185] are given as

$$A(\alpha) = cosh^{-1}\left(\frac{(\pi - 2\alpha - 2\delta)\Lambda + (4\alpha - \pi + 2\delta)}{(4\alpha - \pi + 2\delta)\sin(\alpha)}\right), \Lambda = \frac{T}{t_0},$$

$$\mu = \frac{(4\pi\alpha - \pi^2 + 2\pi\delta)M}{A(\alpha)T}, k = \frac{A(\alpha)}{M},$$

the decay rate of the error is

$$B(\alpha) = \frac{\pi^2 - 2\pi\alpha - 2\pi\delta}{A(\alpha)},$$

for given Λ and δ, $B(\alpha)$ can be maximized to find the optimal value of α, this is done with Newton's method. For these parameters the error estimate is of the order

$$E_2 = |u_k(\mathbf{x}, t) - u(\mathbf{x}, t)| = O\left(e^{-B(\alpha)M}\right), M \to \infty \tag{2.4.7}$$

The optimal parameters involved in the modified hyperbolic contour C_3 defined by (1.3.18) proposed in [181] are based on the following theorem

Theorem 2.4.2. *[181] Let $u(\mathbf{x}, t)$ be the solution of (2.1.1)-(2.1.3), with $R(\mathbf{x}, z)$ analytic in Σ_β^ω. Let $0 < t_0 < T$,$0 < \theta < 1$, where $\tau = t_0/T$, and $b > 0$ defined by $b = cosh^{-1}(1/(\theta\tau\sin(\delta)))$. Let $\Gamma \subset \Omega_r \subset \Sigma_\beta^\omega$, and let $\omega = \frac{\theta\bar{r}M}{bT}$. Then for the approximate solution $u_k(\mathbf{x}, t)$ defined by (2.1.1)-(2.1.3), with $k = \frac{b}{M} \leq \frac{\bar{r}}{log(2)}$,*

$$|u_k(\mathbf{x}, t) - u(\mathbf{x}, t)| \leq CLe^{\lambda t} l(\rho_r M) e^{-\mu M}\left(\|u_0\| + \|R(\mathbf{x}, z)\|_{\Sigma_\beta^\omega}\right),$$

for $t_0 \leq t \leq T$, where $l(x) = max(1, log(1/x))$, $r > 0$, $\mu = \overline{r}(1 - \theta)/b$,

the error estimate is of order

$$E_3 = |u_k(\mathbf{x}, t) - u(\mathbf{x}, t)| = O\left(l(\rho_r M)e^{-\mu M}\right). \tag{2.4.8}$$

2.5 Chapter summary

In this chapter the linear differential equations are considered with initial and boundary conditions. we proposed Laplace transform local kernel based method for time dependent PDEs. The method is capable to solve time dependent PDEs of integer and fractional order. However, there are some difficulties, for example the Laplace transform is a linear operator and as such cannot handle non-linear terms. The problem of non linearity can be handled by a linearisation process together with a suitable iterative scheme [225]. Since the Laplace transform is a linear operator and can not be applied directly to non-linear equations. So some iterative procedures may be used to linearized the problem.

If the forcing term does not have analytically known Laplace transform, then in that case also the Laplace transform cannot be applied directly. Then we have to find an approximation to forcing term that has an analytically known Laplace transform. In literature the available techniques for finding an approximation to the forcing term are [179]: (i) Least squares approximation. (ii) Completely monotonic functions and Gauss-Laguerre approximation. (iii) Prony's method.

Chapter 3

Laplace transform local kernel based method for integer and fractional order diffusion equations

3.1 Introduction

Diffusion models of fraction order are very important tools for characterizing anomalous diffusion. In a diffusion model, the diffusion process becomes slower by replacing time derivative by the fractional derivative [226]. It is shown in [227] that flow of fluid in aquifer may be more accurately modeled by fractional order diffusion as compared to usual diffusion. Anomalous diffusion phenomena have been observed in various scientific and engineering fields, such as dissipation [228], heat conduction [192], diffusion in porous media [229], turbulence [230], control system and chaos [231, 232]. Fractional derivative have been used to model anomalous phenomena in various fields of sciences and engineering successfully by many researchers [233, 234, 235]. We will validate our method for the following model,

$$\partial_t^{\alpha} u(\mathbf{x},t) = f(\mathbf{x},t) + \mathcal{L}u(\mathbf{x},t),\ \mathbf{x} \in \Omega \subset R^d, d \geq 1, 0 < \alpha < 1, \tag{3.1.1}$$

with initial condition

$$u(\mathbf{x},0)=u_0,\ \mathbf{x}\in\Omega, \tag{3.1.2}$$

and boundary condition

$$\mathcal{B}u(\mathbf{x},t)=g(\mathbf{x},t),\ \mathbf{x}\in\partial\Omega, \tag{3.1.3}$$

where $\mathcal{L}$ is the governing differential operator and $\mathcal{B}$ is the boundary differential operator.

Applying Laplace transform to (3.1.1)-(3.1.3), we have

$$z^{\alpha}\hat{u}(\mathbf{x},z)-z^{\alpha-1}u_0=\hat{f}(\mathbf{x},z)+\mathcal{L}\hat{u}(\mathbf{x},z), \tag{3.1.4}$$

and

$$\mathcal{B}\hat{u}(\mathbf{x},z)=\hat{g}(\mathbf{x},z), \tag{3.1.5}$$

these equation can be simplified as

$$(z^{\alpha}-\mathcal{L})\hat{u}(\mathbf{x},z)=\hat{r}(\mathbf{x},z), \tag{3.1.6}$$

$$\mathcal{B}\hat{u}(\mathbf{x},z)=\hat{g}(\mathbf{x},z), \tag{3.1.7}$$

where $\hat{f}(\mathbf{x},z)$ and $\hat{g}(\mathbf{x},z)$ are the corresponding Laplace transforms of $f(\mathbf{x},t)$ and $g(\mathbf{x},t)$, and $\hat{r}(\mathbf{x},z)=z^{\alpha-1}u_0+\hat{f}(\mathbf{x},z)$. After discretization of the operators $\mathcal{L}$ and $\mathcal{B}$ by localized meshless method the system (3.1.6)-(3.1.7) is solved for each point along the contour of integration z. Then the solution $u(\mathbf{x},t)$ of problem (3.1.1)-(3.1.3) can be obtained by the inverse Laplace transform

$$u(\mathbf{x},t)=\frac{1}{2\pi i}\int_{\sigma-i\infty}^{\sigma+i\infty}e^{zt}\hat{u}(\mathbf{x},z)dz=\frac{1}{2\pi i}\int_{\Gamma}e^{zt}\hat{u}(\mathbf{x},z)dz,\quad \sigma>\sigma_0, \tag{3.1.8}$$

Using either of the parabolic or hyperbolic contour defined by (1.3.15), (1.3.17), or (1.3.18) the integral representation (3.1.8), becomes

$$u(\mathbf{x},t)=\frac{1}{2\pi i}\int_{-\infty}^{\infty}e^{z(\zeta)t}\hat{u}(\mathbf{x},z(\zeta))\acute{z}(\zeta)d\zeta, \tag{3.1.9}$$

The approximation of (3.1.9) by trapezoidal rule with uniform step size k, and quadrature points $z_j = z(\zeta_j), \zeta_j = jk$, is given as

$$u_k(\mathbf{x}, t) = \frac{k}{2\pi i} \sum_{j=-M}^{M} e^{z_j t} \hat{u}(\mathbf{x}, z_j) \acute{z}_j. \tag{3.1.10}$$

3.2 Numerical problems

We apply our proposed method to the diffusion problems to validate our method. We are using The multiquadrics $\phi(r, \varepsilon) = (1 + (\varepsilon r)^2)^{1/2}$, Inverse multiquadrics $\phi(r, \varepsilon) = 1/(1 + (\varepsilon r)^2)^{1/2}$, and Gussian $\phi(r, \varepsilon) = e^{-(\varepsilon r)^2}$ radial kernel contains shape parameter ε, and solution accuracy depends on parameter ε. We use the Uncertainty principal [223] to select the shape parameter for good accuracy.

To show the accuracy of the method and for comparison two kinds of error norms are used, maximum absolute error(L_∞) and Root mean square error (RMS) defined by

$$L_\infty = \|u_k(\mathbf{x}_i, t) - u(\mathbf{x}_i, t)\|_\infty = \max_{1 \le i \le N} (|u_k(\mathbf{x}_i, t) - u(\mathbf{x}_i, t)|)$$

$$RMS = \sqrt{\frac{\sum_i^N (u_k(\mathbf{x}_i, t) - u(\mathbf{x}_i, t))^2}{N}}$$

Problem 3.2.1. *Here we consider the one-dimension diffusion equation with Dirichlet boundary conditions,*

$$\begin{aligned} &\frac{\partial u}{\partial t} = \frac{\partial^2 u}{\partial x^2} - e^x t(t-2), \ t > 0, \ x \in [0, 1], \\ &u(x, 0) = 0, \ t = 0, \ x \in [0, 1], \\ &u(0, t) = t^2, \ u(1, t) = et^2, \ t > 0. \end{aligned} \tag{3.2.1}$$

The exact solution of this problem is $u(x, t) = e^x t^2$, and the boundary conditions are used according to the exact solution. The problem is solved over the domain

$0 \leq x \leq 1$ at $t = 1$. Different quadrature points are used along the parabolic C_1 and hyperbolic C_3 contours. These points are generated by MATLAB statement $\zeta = -M : k : M$ for parabolic contour C_1, and hyperbolic contour C_3. The parameters used are $\theta = 0.1, \delta = 0.3812, r = 0.3431, \omega = 2, c = 0.1, t_0 = 0.5$ and $T = 5$. The other optimal parameters are given in (1.3.15) and (1.3.18) for both contours parabolic C_1 and hyperbolic C_3 respectively. The L_∞ error and error estimates for both the contours parabolic and hyperbolic are shown in Table 3.1 and 3.2 respectively. Numerical and exact solution are shown in Figure 3.1. Absolute error versus quadrature points along three different contours C_1, C_2, C_3, and for three types of radial kernels are shown in the Figure 3.2-3.3. Various number of points N in the global domain Ω and n in the local domain Ω_i are used. The shape parameter is optimized using the uncertainty principle [223]. This method give us almost exact solution in time, error occurs only in spatial discretization. So we can approximate diffusion equation very accurately in time without any time instability issue. The local nature of the method make it more attractive for such type of problems.

M	N	n	L_∞(error)	E_1
25	20	5	0.1003	2.6311e-008
30	25	6	0.0069	8.0197e-010
40	30	7	6.0546e-005	7.4509e-013
50	40	8	6.0438e-005	6.9225e-016
60	45	10	4.9352e-005	6.4315e-019

Table 3.1: Numerical solution obtained by the present method using the parabolic contour C_1 at $t = 1$, and $1e12 < \kappa < 1e18$.

M	N	n	L_∞ (error)	E_3
8	15	4	0.0267	0.9335
10	20	5	0.0064	0.5138
15	25	6	1.9476e-004	0.1138
20	30	7	7.5416e-005	0.0249
30	32	8	3.1184e-005	0.0012

Table 3.2: Numerical solution obtained by the present method using the hyperbolic contour C_3 at $t = 1$, and $1e12 < \kappa < 1e18$.

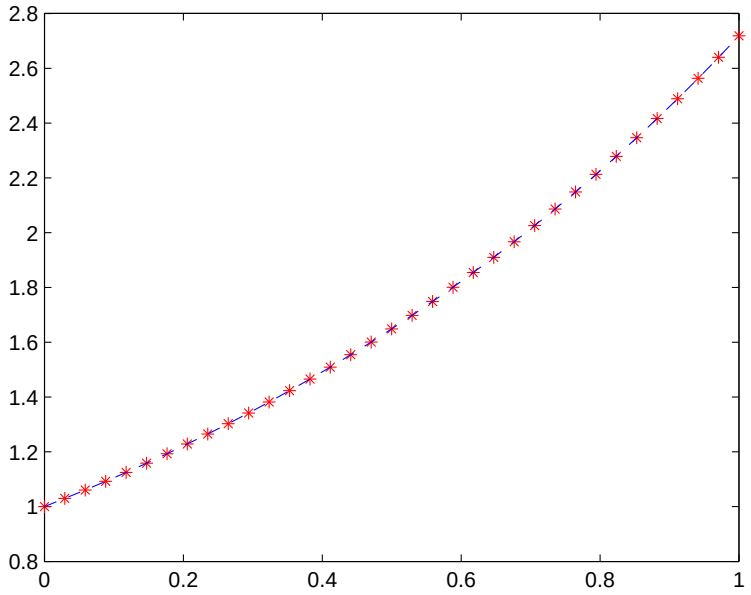

Figure 3.1: Plot of numerical and exact solution for the problem 3.2.1 obtained by the present method at $t = 1$.

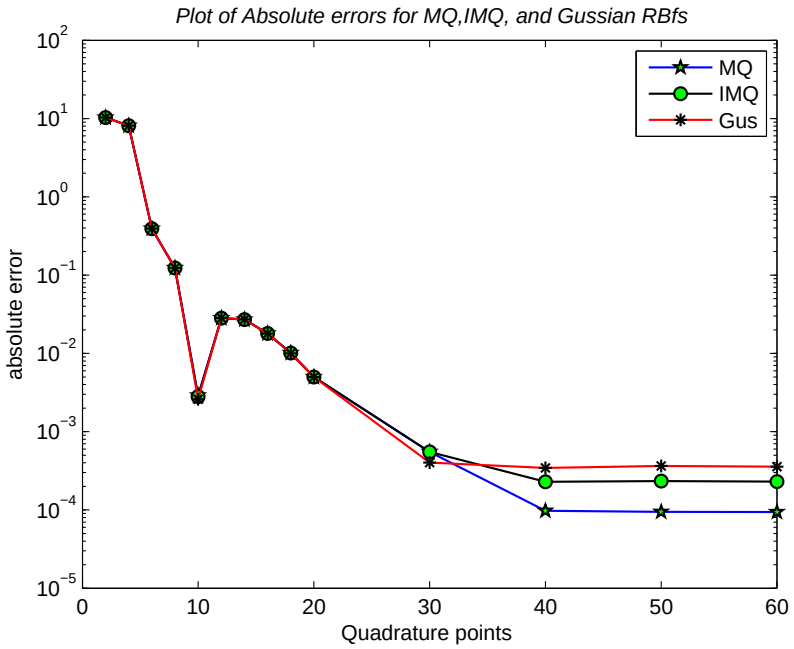

Figure 3.2: Absolute error versus number of quadrature points along the contour C_3, using $N = 35$ and $n = 10$ uniform interpolation nodes in domain $[0, 1]$ and the local sub-domain respectively at $t = 1$. Three different radial kernels Multiquadrics (MQ), Inverse multiquadrics (IMQ), and Gussian (Gus) are used.

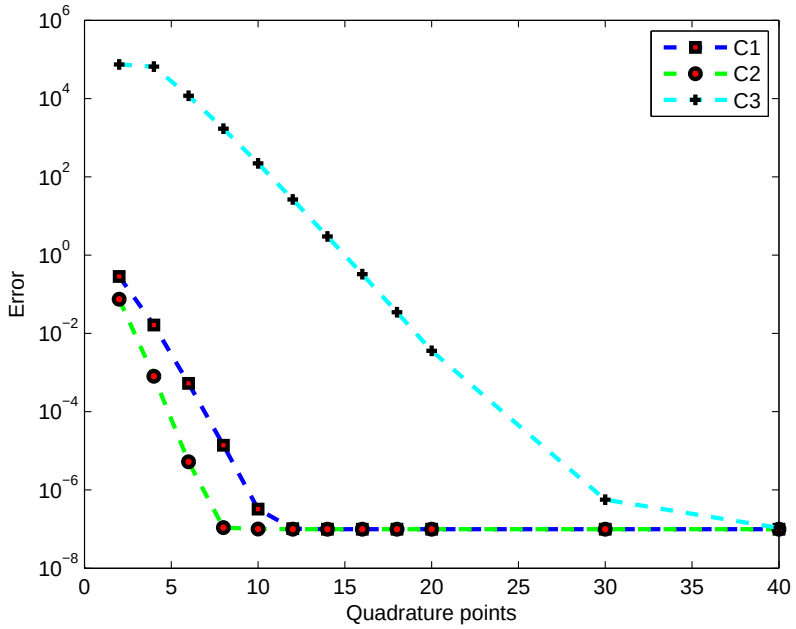

Figure 3.3: Absolute error versus number of quadrature points using $N = 20$, and $n = 5$ uniform interpolation nodes in domain $[0, 1]$ and the local sub-domain respectively at $t = 0.1$, using MQ RBFs for three different contours of integration.

Problem 3.2.2. *In our second test problem we consider the diffusion equation [64],*

$$\begin{aligned} &\frac{\partial u(x,y,t)}{\partial t} = \nabla^2 u(x,y,t),\ t > 0,\ (x,y) \in \Omega, \\ &u(x,y,0) = 1,\ t = 0,\ (x,y) \in \Omega, \\ &u(x,y,t) = 0,\ t > 0\ (x,y) \in \partial\Omega. \end{aligned} \tag{3.2.2}$$

The exact solution of this problem is given by

$$u(x,y,t) = \frac{16}{\pi^2} u_{ana}(x,t) u_{ana}(y,t) \tag{3.2.3}$$

with $\xi = x, y,$

$$u_{ana}(\xi,t)=\sum_{i=0}^{\infty}\frac{(-1)^i\exp(-(2i+1)^2\pi^2 t)\cos((2i+1)\pi\xi)}{2i+1}. \tag{3.2.4}$$

Here we tested our method for the two dimensional diffusion problem in the domain $[-0.5,0.5]^2$. Two types of centers, i.e uniform and non-uniform centers are chosen in the domain Ω. In case of C_1 non-uniform centers are selected, while for C_3 uniform centers are selected. A sample uniform and non-uniform centers are shown in Figure 3.4. The result for both types of centers using the parabolic contour C_1 and hyperbolic contour C_3 are given in Table 3.3 and 3.4 respectively. The method is tested for different number of points N in the global domain Ω and n in the local domain Ω_i. The parameters used are $\theta=0.1,\delta=0.3812,r=0.3431,\omega=2,c=0.1,t_0=0.5$ and $T=5$. The other optimal parameters are given in (1.3.15) and (1.3.18) for both contours parabolic C_1 and hyperbolic C_3 respectively. Similar performance is observed like one we observed in Problem 3.2.1. So the proposed method is best for approximating diffusion equation in multi dimensions as well. The approximate solution profiles for various times are shown in Figure 3.5.

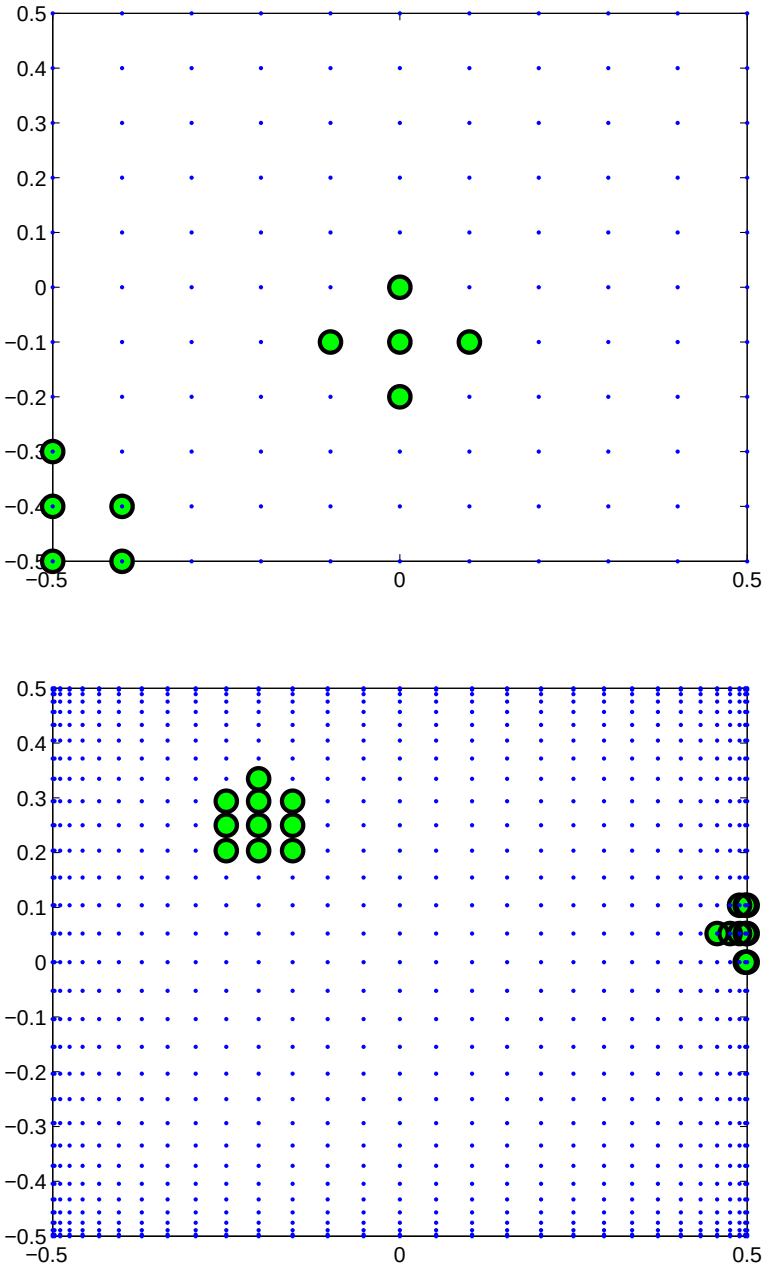

Figure 3.4: The 11×11 uniform, 31×31 nonuniform (Cheb) nodes arrangement, and a sample of $n = 5,\ 10$ interior and boundary local sub-domain nodes arrangement in domain $[-0.5, 0.5]^2$.

M	N	n	L_∞(error)	E_1
5	15	7	0.0105	0.0305
8	20	8	1.6265e-005	0.0038
10	25	9	7.0138e-009	9.2908e-004
15	30	10	1.1414e-009	2.8319e-005
20	35	12	6.4921e-010	8.6319e-007
25	40	15	3.7553e-010	2.6311e-008

Table 3.3: Numerical solution obtained by the present method using non-uniform nudes and the parabolic contour C_1 at $t = 1$, and $1e12 < \kappa < 1e16$.

t	L_∞ (error)	ε	κ
0.01	0.1217	4.6000	2.0794e+014
0.1	0.0118	4.6000	2.0794e+014
1	2.3246e-008	4.6000	6.5857e+014

Table 3.4: Numerical solution for the choice of $N = 32 \times 32$ uniform nodes in the domain $[-0.5, 0.5]^2$ and $n = 12$ nodes in the local sub-domain, and $1e12 \leq \kappa \leq 1e16$, along the contour C_3.

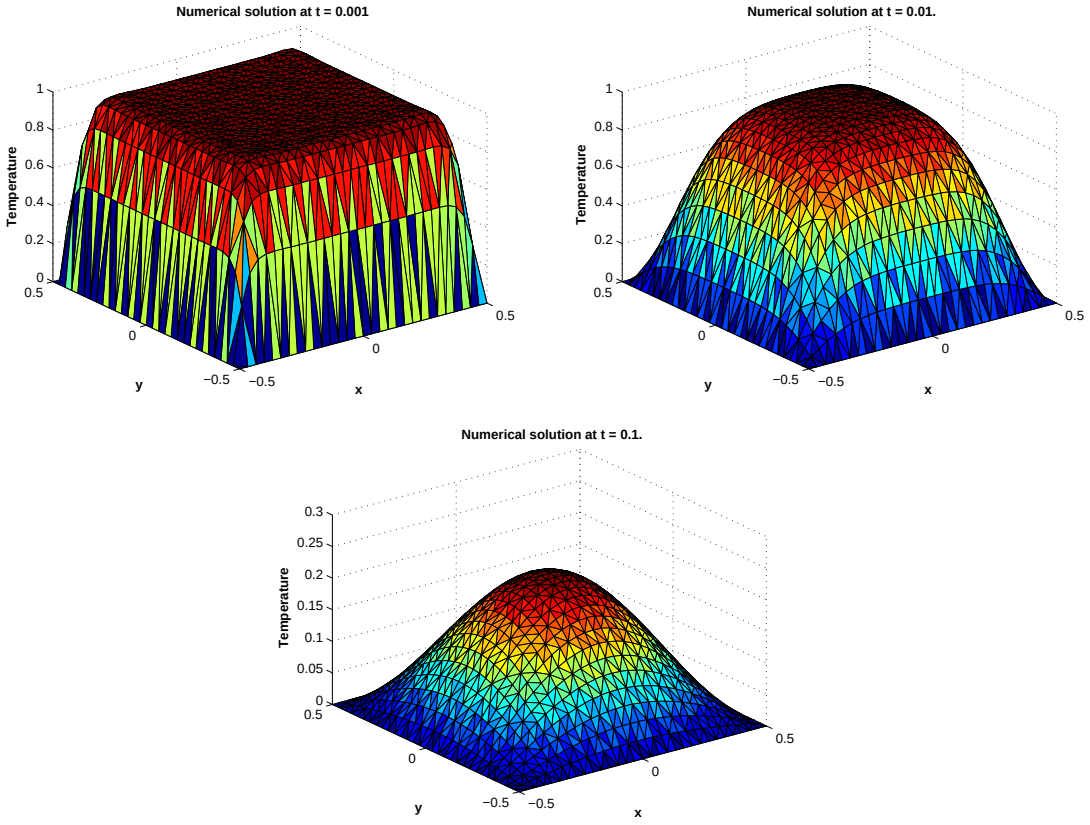

Figure 3.5: The analytical and numerical temperatures at time $t = 0.001,\ 0.01,\ \ 0.1,$ from left to right.

Problem 3.2.3. *We consider one-dimensional PDE [51]*

$$\begin{aligned} &\frac{\partial^\alpha u(x,t)}{\partial t^\alpha} + u(x,t) = \frac{\partial^2 u(x,t)}{\partial x^2} + f(x,t),\ t > 0,\ x \in [0,2],\ 0 < \alpha < 1 \\ &u(x,0) = 0,\ x \in [0,2], \\ &u(0,t) = 0,\ u(2,t) = 0. \end{aligned} \tag{3.2.5}$$

Where $f(x,t) = \frac{2}{\Gamma(3-\alpha)} x(2-x)t^{2-\alpha} + t^2 x(2-x) + 2t^2$. Analytic solution for this problem is $u(x,t) = x(2-x)t^2$ and $\alpha = 0.7$. The computation is performed over the

domain $0 \leq x \leq 2$. We select $N = 30$ uniformly distributed centers in the domain and $n = 5$ centers in the local overlapping sub-domains. We used the uncertainty principal from the theory of RBFs [223] to keep the condition number κ in interval $1e12 \leq \kappa \leq 1e16$ to get the good value of shape parameter ε. The numerical results are given in Figure 3.6 and Table 3.5. We compared our results with other global meshless method [51] for fractional order diffusion equation. It is observed that results of the global meshless method [51] even for a small time step are not good enough from the results of our local meshless method. The numerical results for the three types of contour of integration C_1 (1.3.15), C_2 (1.3.17) and C_3 (1.3.18) respectively are shown in Figure 3.6. The results for various quadrature points for the three contours are given in Figure 3.6. For C_1 and C_2 convergence is achieved for fever number of quadrature points, while using C_3 the same accuracy achieved is for comparatively larger number of quadrature points.

t	L_∞(error)	ε	κ
0.1	2.7904e-008	0.4000	6.2250e+012
0.5	1.0579e-006	0.4000	6.2250e+012
1.0	8.3717e-006	0.4000	6.2250e+012
[51]	δt	L_∞ (error)	error rate
	0.1	8.3e-003	–
	0.05	3.4e-003	$2.44 \approx (0.1/0.05)^{1.3}$
	0.01	4.3e-004	$8.10 \approx (0.05/0.01)^{1.3}$
	0.005	1.7e-004	$2.52 \approx (0.01/0.005)^{1.3}$

Table 3.5: Numerical solution for the choice of $N = 30$ uniform nodes in the domain $[0, 2]$ and $n = 5$ nodes in the local sub-domain, $\alpha = 0.7$, and $1e12 \leq \kappa \leq 1e16$. The results are calculated along the contour C_3 for $M = 50$.

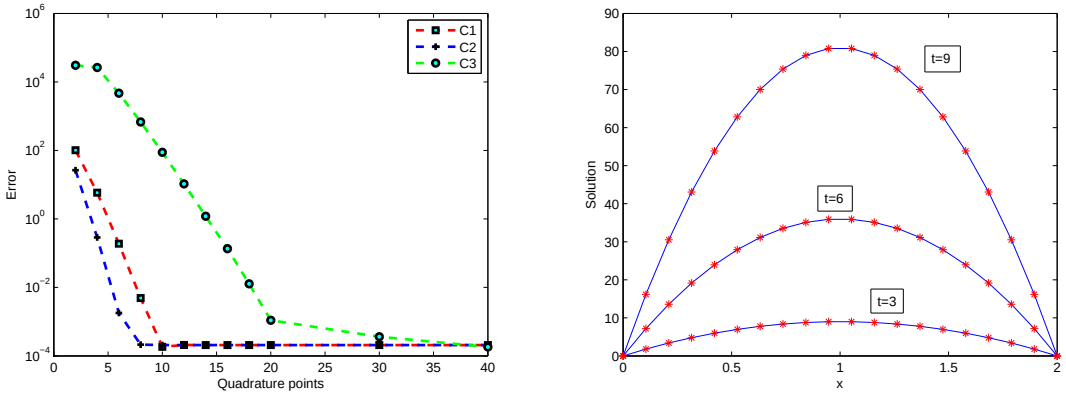

Figure 3.6: Absolute error versus number of quadrature points using $N = 20$, and $n = 5$ uniform interpolation nodes in domain $[0, 2]$ and the local sub-domain respectively at $t = 3$. In the second plot profiles of exact and numerical solution are shown at different times.

Problem 3.2.4. *Here we consider the PDE [128]*

$$\begin{aligned} &\partial_t^{\alpha} u(x,y,t) + u(x,y,t) = \Delta u(x,y,t) + f(x,y,t),\ 0 < \alpha < 1, \\ &u(x,y,0) = 0,\ t = 0,\ 0 \le x, y \le 2, \\ &u(x,y,t) = t^2 \sin\frac{\pi x}{2} \sin\frac{\pi y}{2},\ x, y \in \partial\Omega, \end{aligned} \tag{3.2.6}$$

where

$$f(x,y,t) = \left[\frac{2t^{2-\alpha}}{\Gamma(3-\alpha)} + \left(1 + \frac{\pi^2}{2}\right) t^2\right] \sin\frac{\pi x}{2} \sin\frac{\pi y}{2},$$

and

$$u(x,y,t) = t^2 \sin\frac{\pi x}{2} \sin\frac{\pi y}{2},$$

as analytic solution. To test our method for two-dimensional diffusion equation, we consider the square domain $[0, 2]^2$. Further we select uniform nodes in the domain and $\alpha = 0.5$. We choose various size n centers in each local sub-domains. We compared

our result with an other local meshless method [128] using time stepping procedure. We see that the present Laplace transform local kernel based method produced better results. Graphs of numerical and exact solution are shown in the Figure 3.7

N	RMS (n = 5)	RMS (n = 9)	RMS (n = 16)	RMS (n = 25)
11 ×11	2.20e-003	3.11e-004	6.50e-004	1.58e-004
21 ×21	5.79e-004	1.31e-004	2.42e-005	5.81e-005
41 ×41	9.76e-005	7.42e-005	1.95e-005	1.55e-005
[128]				
11 ×11	2.91e-003	5.44e-003	4.46e-004	3.99e-003
21 ×21	3.59e-003	2.74e-003	3.05e-003	5.32e-003
41 ×41	3.44e-003	2.59e-003	2.96e-003	3.85e-003

Table 3.6: Numerical solution for the choice of uniform nodes in the domain $[0, 2]^2$ at $t = 1$ and $1e10 \leq \kappa \leq 1e16$.

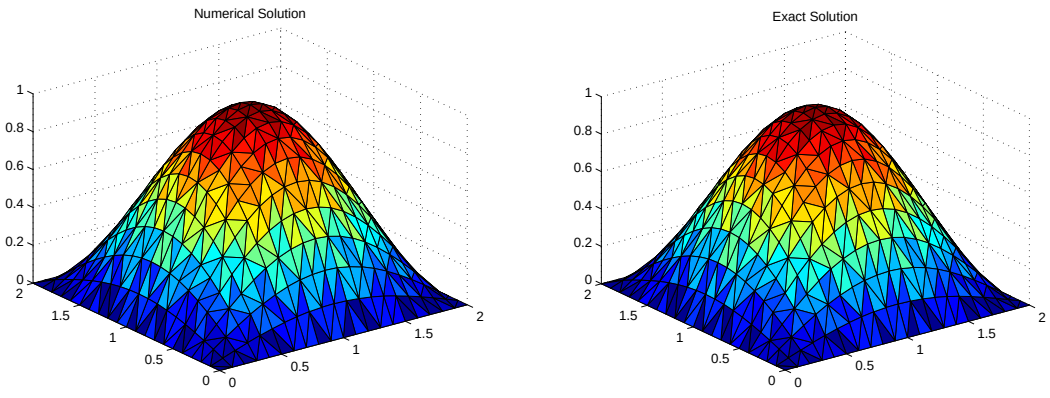

Figure 3.7: Graphs of the numerical and exact solutions for the problem 3.2.4 in the domain $[0, 2]^2$ at $t = 1$.

3.3 Chapter summary

In this chapter, we applied our method to $1-D$ and $2-D$ diffusion problems with time fractional order. The accuracy and performance of the methods is good for solving time fractional diffusion equations. The superiority of our method is demonstrated by comparison with available methods in literature.

Chapter 4

Laplace transform local kernel based method for fractional wave-diffusion equations

4.1 Introduction

Fractional diffusion and wave-diffusion equations can modeled many phenomena such as acoustic, electromagnetic, and mechanical responses. Fractional wave-diffusion equation is considered by many researchers. In [236] the authors obtained the solution of fractional wave-diffusion equation in terms of Wright function. The authors [237] derived the solution of fourth order fractional diffusion wave equation. The general solution of fourth order fractional diffusion wave equation in bounded domain was discussed in [238]. The general analytical technique of fractional wave diffusion system subjected to a non-homogeneous field are discussed in [239]. Other works related to fractional diffusion and wave diffusion can be found in [240, 241, 10, 242, 243]. Here the proposed Laplace transform local kernel based method is tested for time fractional differential equation of order $1 < \alpha < 2$ of the form

$$\partial_t^\alpha u(\mathbf{x},t) + \mathcal{L}u(\mathbf{x},t) = f(\mathbf{x},t),\ \mathbf{x} \in \Omega \subset \mathbb{R}^d,\ d \geq 1. \tag{4.1.1}$$

with the initial conditions

$$u(\mathbf{x},0)=u_0(\mathbf{x}),\ u_t(\mathbf{x},0)=u_1(\mathbf{x}),\ \mathbf{x}\in\Omega, \tag{4.1.2}$$

and the boundary conditions

$$\mathcal{B}u(\mathbf{x},t)=g_1(\mathbf{x},t),\ \mathbf{x}\in\partial\Omega, \tag{4.1.3}$$

where $\mathcal{L}$ is a linear spatial differential operator and $\mathcal{B}$ is boundary operator. Applying the Laplace transform to equation (4.1.1)-(4.1.3), we get

$$\left[z^{\alpha}\hat{u}(\mathbf{x},z)-z^{\alpha-1}u_0-z^{\alpha-2}u_1\right]+\mathcal{L}\{\hat{u}(\mathbf{x},z)\}=\hat{f}(\mathbf{x},z),\ \mathbf{x}\in\Omega, \tag{4.1.4}$$

and

$$\mathcal{B}\{\hat{u}(\mathbf{x},z)\}=\hat{g_1}(\mathbf{x},z),\ \mathbf{x}\in\partial\Omega, \tag{4.1.5}$$

respectively. Thus we have the following system of linear differential equations

$$\left[z^{\alpha}I+\mathcal{L}\right]\{\hat{u}(\mathbf{x},z)\}=\hat{g}(\mathbf{x},z),\ \mathbf{x}\in\Omega, \tag{4.1.6}$$

$$\mathcal{B}\{\hat{u}(\mathbf{x},z)\}=\hat{g_1}(\mathbf{x},z),\ \mathbf{x}\in\partial\Omega, \tag{4.1.7}$$

where

$$\hat{g}(\mathbf{x},z)=z^{\alpha-1}u_0+z^{\alpha-2}u_1+\hat{f}(\mathbf{x},z),$$

After discretization of the operators $\mathcal{L}$ and $\mathcal{B}$ by localized meshless method the system (4.1.6)-(4.1.7) is solved for each point along the contour of integration z. Then the solution $u(\mathbf{x},t)$ of problem (4.1.1)-(4.1.3) can be obtained by the inverse Laplace transform

$$u(\mathbf{x},t)=\frac{1}{2\pi i}\int_{\sigma-i\infty}^{\sigma+i\infty}e^{zt}\hat{u}(\mathbf{x},z)dz=\frac{1}{2\pi i}\int_{\Gamma}e^{zt}\hat{u}(\mathbf{x},z)dz,\quad \sigma>\sigma_0, \tag{4.1.8}$$

Using either of the parabolic or hyperbolic contour defined by (1.3.15), (1.3.17), or (1.3.18) the integral representation (4.1.8), becomes

$$u(\mathbf{x},t)=\frac{1}{2\pi i}\int_{-\infty}^{\infty}e^{z(\zeta)t}\hat{u}(\mathbf{x},z(\zeta))\acute{z}(\zeta)d\zeta, \tag{4.1.9}$$

The approximation of (4.1.9) by trapezoidal rule with uniform step size k, and quadrature points $z_j=z(\zeta_j),\zeta_j=jk$, is given as

$$u_k(\mathbf{x},t)=\frac{k}{2\pi i}\sum_{j=-M}^{M}e^{z_jt}\hat{u}(\mathbf{x},z_j)\acute{z}_j. \tag{4.1.10}$$

4.2 Numerical problems

The proposed method is applied to the diffusion-wave problems in order to validate our hybrid numerical scheme. The multiquadrics $\phi(r,\varepsilon)=(1+(\varepsilon r)^2)^{1/2}$ are used in all our computations. The above algorithm actually due to [223] is used to select the shape parameter ε for obtaining good accuracy.

To show the accuracy of the method and for comparison two kinds of error norms are used, maximum absolute error(L_∞) and Root mean square error (RMS) defined by

$$L_\infty=\|u_k(\mathbf{x}_i,t)-u(\mathbf{x}_i,t)\|_\infty=\max_{1\le i\le N}(|u_k(\mathbf{x}_i,t)-u(\mathbf{x}_i,t)|)$$

$$RMS=\sqrt{\frac{\sum_i^N(u_k(\mathbf{x}_i,t)-u(\mathbf{x}_i,t))^2}{N}}$$

Problem 4.2.1. *Here we apply our proposed numerical method to the one dimensional fractional diffusion-wave equation [244],*

$$\begin{aligned}&\partial_t^\alpha u(x,t)=\partial_{xx}u(x,t)+f(x,t),\ 1<\alpha<2,\\&u(x,0)=0,\ u_t(x,0)=0,\ 0\le x\le 1,\end{aligned} \tag{4.2.1}$$

where $f(x,t) = -2t^2 + x(x-1)\frac{2t^{2-\alpha}}{\Gamma(3-\alpha)}$, and the boundary conditions may be used from the exact solution $u(x,t) = x(x-1)t^2$. The problem is solved over the domain $[0,1]$ at time $t = 1$. We used different quadrature points along the parabolic contour C_1 as well as hyperbolic contour C_3 for computing the solution. These points can be generated by MATLAB statement $\zeta = -M : k : M$ for parabolic contour C_1, and hyperbolic contour C_3 respectively. For the input parameters, $c = 0.1$, $\omega = 2$, $t_0 = 0.5$, $T = 5$, $\theta = 0.1$, $\delta = 0.1541$, and $r = 0.1387$, the other optimal parameters can be obtained using (1.3.15) and (1.3.18) for both the parabolic and hyperbolic contours respectively. The results in term of L_∞ and RMS error norm as well as the error estimates E_1 and E_3 of the method using both the contours C_1 and C_3 are shown in table 4.2. The results are compared with meshfree time stepping method [244]. It is observed that the stable and more accurate results are obtained with Laplace transformed-based localized method. Various number of points N in global domain Ω and n in the local domains Ω_i are used for this problem. The MQ radial basis function with shape parameter which is optimized using the criteria of [223] have been used. This method gives almost exact solution in time, error occurs only in spatial disretization. So we can approximate time fractional partial differential equation very accurately in time without any time in-stability issue which is the main issue of time stepping meshfree methods. The local nature of the method makes it more attractive for solving such types of problems.

$\alpha = 1.5$, $n = 10$, $N = 30$	M	L_∞ (error)	RMS (error)	E_1	C. time(s)
	5	0.3749	0.0125	1.01e-004	0.474173
	7	0.0259	8.63e-004	2.55e-006	0.535634
	10	3.60e-004	1.20e-005	1.02e-008	0.571459
	15	1.30e-005	4.33e-007	1.03e-012	0.730256
	20	1.31e-005	4.36e-007	1.05e-016	1.039483
$\alpha = 1.5$, $M = 15$, $n = 5$	N	L_∞ (error)	RMS (error)	E_1	C. time(s)
	5	3.36e-005	6.73e-006	1.03e-012	0.625325
	10	4.42e-005	4.42e-006	1.03e-012	0.634963
	15	3.39e-005	2.26e-006	1.03e-012	0.685464
	20	6.42e-006	3.21e-007	1.03e-012	0.662561
	30	1.83e-006	6.10e-008	1.03e-012	0.725135
[244] 8.993e-004					

Table 4.1: Numerical solution obtained by the present method in terms of L_∞, RMS error norms, and error estimates E_1 and E_3 for the contours C_1, and C_3 respectively, corresponding to problem 4.2.1 when $\alpha = 1.5$.

$\alpha = 1.85$, $N = 30$, $n = 5$	M	L_∞(error)	RMS (error)	E_3	C. time(s)
	5	0.4789	0.0160	7.2328	0.413607
	7	0.0209	6.9810e-004	5.9685	0.452323
	10	2.7148e-004	9.0492e-006	4.4187	0.481080
	15	7.8910e-004	2.6303e-005	2.6363	0.554561
	30	5.3436e-005	1.7812e-006	0.5373	1.151794
	40	5.5946e-006	1.8649e-007	0.1836	1.542843
	70	4.1114e-006	1.3705e-007	0.0072	5.494285
	90	4.1206e-006	1.3735e-007	8.1825e-004	11.283902
[244] 4.6589e-004					

Table 4.2: Numerical solution obtained by the present method in terms of L_∞, RMS error norms, and error estimates E_1 and E_3 for the contours C_1, and C_3 respectively, corresponding to problem 4.2.1 when $\alpha = 1.85$.

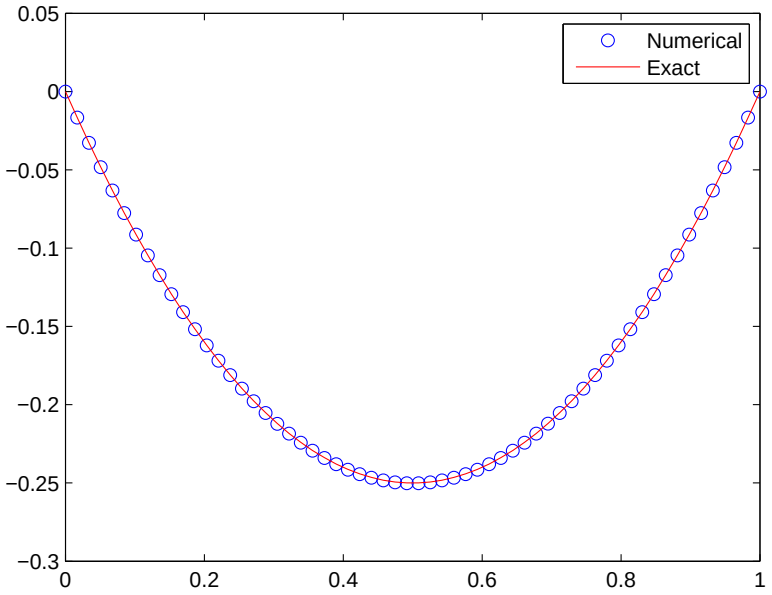

Figure 4.1: Graph of exact and numerical solution corresponding to the problem 4.2.1 obtained with $t = 1, N = 60, n = 20, \alpha = 1.85$.

Problem 4.2.2. *Next we consider the two dimensional fractional diffusion-wave equation,* $1 < \alpha < 2$,

$$\begin{aligned} &\frac{\partial^\alpha u(x,y,t)}{\partial t^\alpha} + u(x,y,t) = \frac{\partial^2 u(x,y,t)}{\partial x^2} + \frac{\partial^2 u(x,y,t)}{\partial y^2} + f(x,y,t), \\ &u(x,y,0) = 0, \;\; u_t(x,y,0) = 0, \;\; 0 \le x, y \le 2, \end{aligned} \tag{4.2.2}$$

where $f(x,y,t) = \left[\frac{2t^{2-\alpha}}{\Gamma(3-\alpha)} + (1 + \frac{\pi^2}{2})t^2\right] \sin(\pi x/2) \sin(\pi y/2)$, and the boundary conditions may be used from the exact solution $u(x,y,t) = t^2 \sin(\pi x/2) \sin(\pi y/2)$. Here we tested our method for two dimensional diffusion-wave equation in square domain $[0,2] \times [0,2]$ at time $t = 1$. The method is tested for different number of points N in global domain Ω and n in local domain Ω_i and quadrature points respectively.

The parameter values $\omega = 2$, $t_0 = 0.5$, $T = 5$, $\theta = 0.1$, $\delta = 0.1541$, and $r = 0.1387$ are used. The other optimal parameters can be obtained using (1.3.18) for the hyperbolic contour C_3. Table 4.3 show the L_∞ and RMS error norm as well as the error estimate E_3 using hyperbolic contour C_3. Similar performance is observed like one we observed in problem 4.2.1. So the proposed method is an excellent alternative for solving the fractional order partial differential equations in multi-dimensions as well.

$\alpha = 1.5$, $N = 40$, $n = 16$	M	L_∞(error)	RMS (error)	E_3	C. time(s)
	7	4.08e-001	1.02e-002	5.9685	4.287867
	10	4.80e-003	1.20e-004	4.4187	6.788077
	20	9.20e-003	2.30e-004	1.5582	23.423006
	30	6.43e-004	1.60e-005	0.5373	52.182227
	40	5.64e-004	1.41e-005	0.1836	97.301914
	70	5.93e-004	1.48e-005	0.0072	344.808994
$\alpha = 1.85$, $M = 70$, $n = 8$	N	L_∞(error)	RMS error	E_3	C. time(s)
	15	1.10e-002	7.34e-004	0.0072	10.500443
	20	8.30e-003	4.13e-004	0.0072	29.435454
	30	4.60e-003	1.54e-004	0.0072	107.499060
	40	2.60e-003	6.52e-005	0.0072	288.507508
	50	1.10e-003	2.17e-005	0.0072	853.904174

Table 4.3: Numerical solution obtained by the present method in terms of L_∞, RMS error norms and error estimate E_3 using the contour C_3, corresponding to problem 4.2.2.

Problem 4.2.3. *Next we consider the two dimensional fractional diffusion-wave equation [245],* $1 < \alpha < 2$*,*

$$\begin{aligned} \frac{\partial^\alpha u(x,y,t)}{\partial t^\alpha} + \frac{\partial u(x,y,t)}{\partial t} = \frac{\partial^2 u(x,y,t)}{\partial x^2} + \frac{\partial^2 u(x,y,t)}{\partial y^2} + f(x,y,t), \\ u(x,y,0) = 0,\ u_t(x,y,0) = 0,\ 0 \le x, y \le 1, \end{aligned} \tag{4.2.3}$$

where $f(x,y,t) = \left(\frac{24t^{4-\alpha}}{\Gamma(5-\alpha)} + 4t^3 + 2t^4\right)\sin(x)\sin(y)$, and the boundary conditions may be used from the exact solution $u(x,y,t) = t^4 \sin(x)\sin(y)$. Here we tested our method for two dimensional diffusion-wave equation in domain $[0,1] \times [0,1]$ at time $t = 1$ and the results are shown in Table 4.4 for the same set of parameters used in problem 4.2.2. We used the hyperbolic contour only in this case. Similar performances are observed like one we observed in problem 4.2.2.

$\alpha = 1.5$, $N = 35$, $n = 14$	M	L_∞ (error)	RMS (error)	E_3	C. time(s)
	7	3.93e-001	1.13e-002	5.9685	4.351443
	10	3.81e-002	1.10e-003	4.4187	5.381004
	20	6.80e-003	1.92e-004	1.5582	17.841618
	30	6.70e-003	1.92e-004	0.5373	39.217162
	40	5.00e-003	1.42e-004	0.1836	77.601300
	70	1.33e-004	3.82e-006	0.0072	267.166041
[245]			1.2762e-004		
$\alpha = 1.95$, $M = 40$, $n = 16$	N	L_∞(error)	RMS (error)	E_3	C. time(s)
	7	2.30e-003	3.22e-004	0.1836	0.775771
	10	1.00e-003	1.02e-004	0.1836	1.466530
	20	7.95e-004	3.97e-005	0.1836	11.869828
	30	3.15e-004	1.05e-005	0.1836	49.813566
	40	7.34e-004	1.83e-005	0.1836	142.222122
[245]			2.3913e-004		

Table 4.4: Numerical solution obtained by the present method in terms of L_∞, RMS error norms and error estimate E_3 using the hyperbolic contour C_3, corresponding to problem 4.2.3.

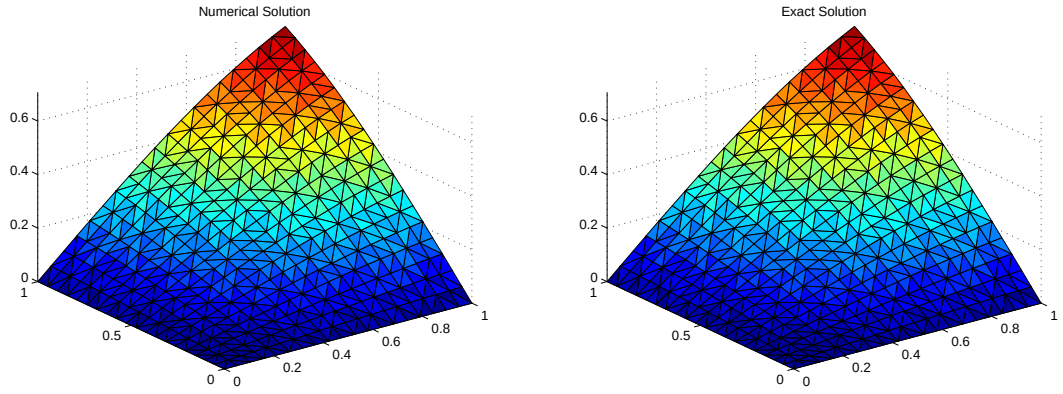

Figure 4.2: The numerical and exact solution when $\alpha = 1.5, N = 20, M = 70, n = 10,$ and $t = 1$.

4.3 Chapter summary

In this chapter, the present method is applied to $1 - D$ and $2 - D$ diffusion-wave equations with time fractional order. The accuracy and performance of the method are excellent for solving time fractional wave-diffusion equations. The method is an alternative for solving time fractional partial differential equations.

Chapter 5

Laplace transform local kernel based method for time fractional telegraph equations

5.1 Introduction

Telegraph equations have applications in many fields such as signal analysis [246], random walk theory [247], wave propagation [248], etc. The time fractional telegraph equation have been considered by many researchers. For example A. Saadatmandi and M. Mohabbati [249, 250], have used Chebshev Tau, and Tau methods for the approximation of telegraph equation. Liu et al [251] considered three types of nonhomogeneous boundary conditions and derived the analytical solution of the nonhomogeneous time-fractional telegraph equation by the method of separation of variables. More work on fractional telegraph equation can be found in the references [252, 191, 6].

We consider time fractional telegraph equation of fractional order $\frac{1}{2} < \alpha \leq 1$ of

the form

$$\frac{\partial^{2\alpha}u(\mathbf{x},t)}{\partial t^{2\alpha}}+\lambda\frac{\partial^{\alpha}u(\mathbf{x},t)}{\partial t^{\alpha}}=\mu\mathcal{L}u(\mathbf{x},t)+f(\mathbf{x},t),\ \mathbf{x}\in\Omega\subset\mathbb{R}^{d},\ d\geq 1. \tag{5.1.1}$$

Subject to initial and boundary conditions

$$u(\mathbf{x},0)=\varphi_1(\mathbf{x}),\ u_t(\mathbf{x},0)=\varphi_2(\mathbf{x}),\ \mathbf{x}\in\Omega, \tag{5.1.2}$$

and

$$\mathcal{B}u(\mathbf{x},t)=g_1(\mathbf{x},t),\ \mathbf{x}\in\partial\Omega, \tag{5.1.3}$$

respectively, where $\mathcal{L}$ is a linear spatial differential operator and $\mathcal{B}$ is boundary operator. Applying the Laplace transform to equation (5.1.1)-(5.1.3), we get

$$\begin{aligned} z^{2\alpha}\hat{u}(\mathbf{x},z)-z^{2\alpha-1}\varphi_1(\mathbf{x})-z^{2\alpha-2}\varphi_2(\mathbf{x})+\lambda\left(z^{\alpha}\hat{u}(\mathbf{x},z)-z^{\alpha-1}\varphi_1(\mathbf{x})\right)& \\ =\mu\mathcal{L}\hat{u}(\mathbf{x},z)+\hat{f}(\mathbf{x},z),\ \mathbf{x}\in\Omega,& \end{aligned} \tag{5.1.4}$$

$$\mathcal{B}\{\hat{u}(\mathbf{x},z)\}=\hat{g_1}(\mathbf{x},z),\ \mathbf{x}\in\partial\Omega. \tag{5.1.5}$$

Where $\hat{f}(\mathbf{x},z)$ and $\hat{g_1}(\mathbf{x},z)$ are the corresponding Laplace transforms of $f(\mathbf{x},t)$ and $g_1(\mathbf{x},t)$ respectively. Thus we have the following system of linear differential equations

$$[z^{2\alpha}I+\lambda z^{\alpha}I-\mu\mathcal{L}]\{\hat{u}(\mathbf{x},z)\}=\hat{g}(\mathbf{x},z),\ \mathbf{x}\in\Omega, \tag{5.1.6}$$

$$\mathcal{B}\{\hat{u}(\mathbf{x},z)\}=\hat{g_1}(\mathbf{x},z),\ \mathbf{x}\in\partial\Omega, \tag{5.1.7}$$

where

$$\hat{g}(\mathbf{x},z)=z^{2\alpha-1}\varphi_1+z^{2\alpha-2}\varphi_2+\lambda z^{\alpha-1}\varphi_1+\hat{f}(\mathbf{x},z).$$

After discretization of the operators $\mathcal{L}$ and $\mathcal{B}$ by localized meshless method the system (5.1.6)-(5.1.7) is solved for each point along the contour of integration z. Then

the solution $u(\mathbf{x},t)$ of problem (5.1.1)-(5.1.3) can be obtained by the inverse Laplace transform

$$u(\mathbf{x},t)=\frac{1}{2\pi i}\int_{\sigma-i\infty}^{\sigma+i\infty}e^{zt}\hat{u}(\mathbf{x},z)dz=\frac{1}{2\pi i}\int_{\Gamma}e^{zt}\hat{u}(\mathbf{x},z)dz,\quad \sigma>\sigma_0, \tag{5.1.8}$$

Using either of the parabolic or hyperbolic contour defined by (1.3.15), (1.3.17), or (1.3.18) the integral representation (5.1.8), becomes

$$u(\mathbf{x},t)=\frac{1}{2\pi i}\int_{-\infty}^{\infty}e^{z(\zeta)t}\hat{u}(\mathbf{x},z(\zeta))\acute{z}(\zeta)d\zeta, \tag{5.1.9}$$

The approximation of (5.1.9) by trapezoidal rule with uniform step size k, and quadrature points $z_j=z(\zeta_j),\zeta_j=jk$, is given as

$$u_k(\mathbf{x},t)=\frac{k}{2\pi i}\sum_{j=-M}^{M}e^{z_jt}\hat{u}(\mathbf{x},z_j)\acute{z}_j. \tag{5.1.10}$$

5.2 Numerical problems

The present method is applied to the time fractional telegraph equation to validate our method. We are using the multiquadrics $\phi(r)=(1+(\varepsilon r)^2)^{1/2}$ contain the shape parameter ε, and solution accuracy depends on parameter ε.

Problem 5.2.1. *Next we apply our numerical to the one dimensional fractional telegraph equation [253],*

$$\frac{\partial^{2\alpha}u(x,t)}{\partial t^{2\alpha}}+\frac{\partial^{\alpha}u(x,t)}{\partial t^{\alpha}}=\frac{1}{2}\frac{\partial^2u(x,t)}{\partial x^2}+f(x,t),\quad 0<x<1,\quad 0<t\leq 1$$

where

$$f(x,t)=\frac{2e^x}{\Gamma(3-2\alpha)}t^{2-2\alpha}+\frac{2e^x}{\Gamma(3-\alpha)}t^{2-\alpha}-\frac{1}{2}t^2e^x,$$

subject to the initial condition $u(x,0) = 0,\ u_t(x,0) = 0,\ \ 0 < x < 1$, *and the boundary conditions*

$$u(0,t) + u_x(0,t) = 2t^2, \quad 0 < t \leq 1,$$

$$u(1,t) - \frac{1}{2}u_x(1,t) = \frac{et^2}{2}, \quad 0 < t \leq 1,$$

with exact solution $u(x,t) = e^x t^2$. The problem is solved over the domain $0 \leq x \leq 1$ at $t = 1$. Different quadrature points are used along the parabolic C_1 and hyperbolic C_2 contours. These points are generated by MATLAB statement $\zeta = -M : k : M$ for parabolic contour C_1, and for hyperbolic contour C_3. The parameters used are $\theta = 0.1, \delta = 0.1541, r = 0.1387, \omega = 2, c = 0.1, t_0 = 0.5$ and $T = 5$. The other optimal parameters are given in (1.3.15) and (1.3.18) for both contours parabolic C_1 and hyperbolic C_3 respectively. The L_∞ error and error estimates using different fractional order $\alpha = 0.64, 0.8, 0.96$ for both the contours parabolic and hyperbolic are shown in 5.1 and 5.2 respectively. Various number of points N in the global domain Ω and n in the local domain Ω_i are used. The shape parameter is optimized using the uncertainty principle [223]. This method give us almost exact solution in time, error occurs only in spatial discretization. So we can approximate diffusion equation very accurately in time without any time instability issue. The local nature of the method make it more attractive for such type of problems.

$\alpha = 0.64$	M	N	n	L_∞ (error)	E_1
	30	20	4	7.6635e-004	8.0197e-010
	50	35	5	4.7424e-004	6.9225e-016
	70	40	6	9.4806e-004	5.9754e-022
	90	50	7	2.5399e-004	5.1579e-028
[253] 7.77e-005					
$\alpha = 0.8$	M	N	n	L_∞ (error)	E_1
	30	20	4	0.0014	8.0197e-010
	50	35	5	4.0083e-004	6.9225e-016
	70	40	6	7.8212e-004	5.9754e-022
	90	50	7	1.6965e-004	5.1579e-028
[253] 7.60e-005					
$\alpha = 0.96$	M	N	n	L_∞ (error)	E_1
	30	20	4	0.0020	8.0197e-010
	50	35	5	3.4758e-004	6.9225e-016
	70	40	6	6.6001e-004	5.9754e-022
	90	50	7	1.1800e-004	5.1579e-028
[253] 2.10e-004					

Table 5.1: The maximum absolute error in our method and in [253] corresponding to problem 5.2.1 along the contour C_1

$\alpha = 0.64$	M	N	n	L_∞ (error)	E_3
	30	20	4	3.5156e-004	0.5373
	50	35	5	4.7451e-005	0.0625
	70	40	6	1.1875e-004	0.0072
	90	60	7	2.0301e-004	8.1825e-004
[253] 7.77e-005					
$\alpha = 0.8$	M	N	n	L_∞	E_3
	30	20	4	1.6778e-004	0.5373
	50	35	5	2.7378e-005	0.0625
	70	40	6	7.4370e-005	0.0072
	90	60	7	1.3771e-004	8.1825e-004
[253] 7.60e-005					
$\alpha = 0.96$	M	N	n	L_∞	E_3
	30	20	4	1.9573e-004	0.5373
	50	35	5	1.6840e-005	0.0625
	70	40	6	4.7542e-005	0.0072
	90	60	7	9.5745e-005	8.1825e-004
[253] 2.10e-004					

Table 5.2: The maximum absolute error in our method and in [253] corresponding to problem 5.2.1 along the contour C_3

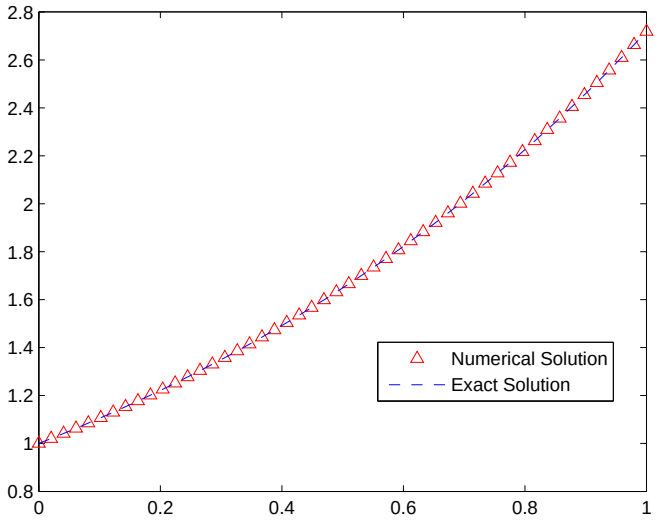

Figure 5.1: Numerical and exact solution corresponding to the problem 5.2.1 when $N = 50, n = 7, M = 100, \alpha = 0.64$.

Problem 5.2.2. *Next we consider the one dimensional telegraph equation with* $\alpha = \frac{2}{3}$,

$$\frac{\partial^{2\alpha} u(x,t)}{\partial t^{2\alpha}} + \frac{\partial^{\alpha} u(x,t)}{\partial t^{\alpha}} = \frac{\partial^2 u(x,t)}{\partial x^2} + f(x,t), \quad 0 < x < 1, \quad 0 < t \leq 1$$

where

$$f(x,t) = 6\sin(x+1)\left(\frac{t^{3-2\alpha}}{\Gamma(4-2\alpha)} + \frac{t^{3-\alpha}}{\Gamma(4-\alpha)}\right) + \sin(x+1)(t^3+1),$$

subject to the initial condition $u(x,0) = \sin(x+1),\ u_t(x,0) = 0, \quad 0 < x < 1$, *and the boundary conditions*

$$u(0,t) = \sin(1)(t^3+1), \quad 0 < t \leq 1,$$

$$u(1,t) + 3u_x(1,t) = (t^3+1)(\sin(2) + 3\cos(2)), \quad 0 < t \leq 1,$$

Here we tested our method for one dimensional Telegraph equation in domain $[0, 1]$ at time $t = 1$ and the results are shown in table 5.3. We used the same parabolic and hyperbolic contours as discussed in problem 5.2.1. Similar performance is observed like one we observed in problem 5.2.1. So the proposed method is an excellent alternative for solving the fractional order telegraph equations in multi-dimensions as well.

$\alpha = \frac{2}{3}$	M	N	n	L_∞ (error)	E_1
	30	20	4	0.0348	8.0197e-010
	50	30	5	1.0965e-005	6.9225e-016
	70	35	6	7.2333e-005	5.9754e-022
	90	45	7	1.1699e-004	5.1579e-028
$\alpha = \frac{2}{3}$	M	N	n	L_∞ (error)	E_3
	30	20	4	0.0867	0.5373
	50	30	5	0.0061	0.0625
	70	35	6	3.3031e-004	0.0072
	90	45	7	1.2168e-004	8.1825e-004

Table 5.3: Numerical solution corresponding to problem 5.2.2 at $t = 1$ along the contour C_1 and C_3

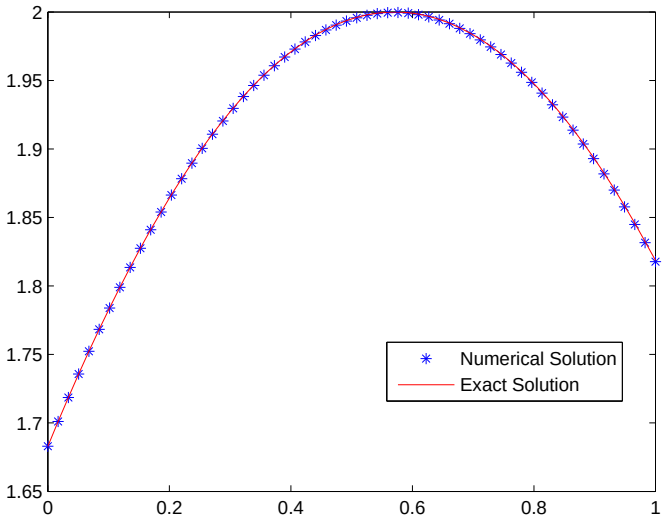

Figure 5.2: Numerical and exact solution corresponding to the problem 5.2.2 when $N = 60, n = 10, M = 90, \alpha = \frac{2}{3}$.

Problem 5.2.3. *As a third example we consider the one dimensional telegraph equation with* $\alpha \in (1, 2]$, *[254]:*

$$\frac{\partial^\alpha u(x,t)}{\partial t^\alpha} + \frac{\partial^{\alpha-1} u(x,t)}{\partial t^{\alpha-1}} + u(x,t) = \pi \frac{\partial^2 u(x,t)}{\partial x^2} + f(x,t), \quad 0 < x < 1, \quad 0 < t \leq 1,$$

where

$$f(x,t) = 6(\sin(x))^2 \left(\frac{t^{3-\alpha}}{\Gamma(4-\alpha)} + \frac{t^{4-\alpha}}{\Gamma(5-\alpha)} + \frac{t^3}{6} \right) - 2\pi t^3 \cos(2x),$$

subject to the initial condition $u(x,0) = u_t(x,0) = 0, \quad 0 < x < 1$, and the boundary conditions are chosen according to the exact solution $u(x,t) = t^3(\sin(x))^2$. Here we tested our method for one dimensional telegraph equation in domain $[0, 1]$ at time $t = 1$. We used the same parabolic and hyperbolic contours and the same optimal parameters as discussed in problem 5.2.1 and problem 5.2.2. The absolute errors and

error estimtes for both the contours C_1 and C_3 are shown in table 5.4 using fractional order $\alpha = 1.25, 1.5, 1.75, 1.95$. It is observed that as we increase the value of α the absolute error dercreases. A clear improvement is observed as compared to [254]. So the proposed method is an excellent alternative for solving the fractional order telegraph equations.

M	N	n	$\alpha = 1.25$	$\alpha = 1.5$	$\alpha = 1.75$	$\alpha = 1.95$	E_1
30	20	4	0.1067	0.1067	0.1067	0.1067	8.0197e-010
50	30	5	1.1856e-005	1.1587e-005	1.1282e-005	1.1020e-005	6.9225e-016
70	35	6	1.0408e-005	1.0345e-005	1.0277e-005	1.0219e-005	5.9754e-022
90	40	7	1.0434e-005	1.0015e-005	9.5282e-006	9.0990e-006	5.1579e-028
M	N	n	$\alpha = 1.25$	$\alpha = 1.5$	$\alpha = 1.75$	$\alpha = 1.95$	E_3
30	20	4	2.9430e-004	2.8274e-004	2.6916e-004	2.5397e-004	0.5373
50	30	5	1.2013e-005	1.1741e-005	1.1428e-005	1.1092e-005	0.0625
70	35	6	1.0408e-005	1.0345e-005	1.0276e-005	1.0211e-005	0.0072
90	40	7	1.0434e-005	1.0015e-005	9.5234e-006	8.9734e-006	8.1825e-004

Table 5.4: Numerical solution corresponding to problem 5.2.3 at $t = 1$ along the contours C_1 and C_3.

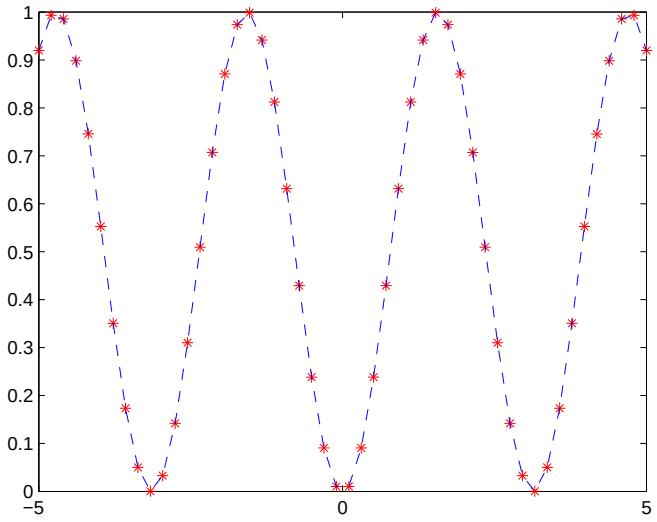

Figure 5.3: Numerical and exact solution corresponding to the problem 5.2.3 over the domain $[-5, 5]$ when $N = 50, n = 6, M = 30, \alpha = 1.1$.

5.3 Chapter summary

In this chapter, the proposed method is applied to fractional telegraph equations. We tested our method for 1-D telegraph equations with time fractional order. It is observed that the proposed Laplace transform local kernel based method produced accurate results.

Chapter 6

Laplace transform local kernel based method for partial integro-differential equations

6.1 Introduction

In this chapter the following partial integro-differential equation is approximated by the method discussed in chapter 2 [255]

$$u_t(\mathbf{x},t) - \int_0^t \beta(t-s)\mathcal{L}u(\mathbf{x},s)ds = f(\mathbf{x},t), \quad \mathbf{x}\in\Omega\subset\mathbb{R}^d, \quad d\geq 1 \quad t>0, \tag{6.1.1}$$

subject to the initial condition

$$u(\mathbf{x},0) = u_0, \mathbf{x}\in\Omega \tag{6.1.2}$$

and boundary conditions given by

$$\mathcal{B}u(\mathbf{x},t) = g_1(\mathbf{x},t), \mathbf{x}\in\partial\Omega, \tag{6.1.3}$$

where $\mathcal{L}$ is a linear spatial operator, $\mathcal{B}$ is a boundary operator and β is defined by

$$\beta(t) = \frac{t^{-1/2}}{\Gamma(1/2)}, \tag{6.1.4}$$

which satisfies

$$\int_0^\tau \int_0^t \beta(t-\tau)\chi(\tau)d\tau\chi(t)dt \geq 0, \forall\ \tau > 0, \quad \chi \in C([0,\tau]). \tag{6.1.5}$$

Equations of the form (6.1.1) arise in viscoelastic phenomena [256], population dynamics, heat conduction [257, 258] etc. The kernel function in these equations becomes weakly singular at the origin [259]. This behavior of the kernel function in visco-elasticity is of particular interest, because when the boundary data is discontinuous it might smooth the solution [260]. Recently great attention has been paid to the approximation of partial integro differential equations (PIDEs). The authors in [261, 262, 263, 264, 259] solved PIDEs using finite element and finite difference methods. In [265], analysis and accurate numerical method is developed for the numerical approximation of such type of equations. The authors in [266, 267] solved hyperbolic and parabolic PIDEs respectively using spline collocation methods. Time discretization scheme was used by Huang for approximating parabolic PIDE [268]. Here we apply the Laplace transform local kernel based method to (6.1.1)-(6.1.3).

Taking Laplace transform of equations (6.1.1)-(6.1.3), we get

$$z\hat{u}(\mathbf{x},z) - u_0 - \beta(z)\mathcal{L}\hat{u}(\mathbf{x},z) = \hat{f}(\mathbf{x},z), \mathbf{x} \in \Omega, \tag{6.1.6}$$

$$\mathcal{B}\{\hat{u}(\mathbf{x},z)\} = \hat{g}_1(\mathbf{x},z),\ \mathbf{x} \in \partial\Omega. \tag{6.1.7}$$

Thus, we have the following system of equations

$$(zI - \beta(z)\mathcal{L})\hat{u}(\mathbf{x},z) = \hat{g}(\mathbf{x},z), \mathbf{x} \in \Omega, \tag{6.1.8}$$

$$\mathcal{B}\{\hat{u}(\mathbf{x},z)\} = \hat{g}_1(\mathbf{x},z),\ \mathbf{x} \in \partial\Omega, \tag{6.1.9}$$

where

$$\hat{g}(\mathbf{x}, z) = u_0 + \hat{f}(\mathbf{x}, z), \tag{6.1.10}$$

and then the solution $u(\mathbf{x}, t)$ of problem (6.1.1)-(6.1.3) can be obtained by the inverse Laplace transform

$$u(\mathbf{x}, t) = \frac{1}{2\pi i} \int_{\sigma - i\infty}^{\sigma + i\infty} e^{zt} \hat{u}(\mathbf{x}, z) dz = \frac{1}{2\pi i} \int_{\Gamma} e^{zt} \hat{u}(\mathbf{x}, z) dz, \quad \sigma > \sigma_0, \tag{6.1.11}$$

Using either of the parabolic or hyperbolic contour defined by (1.3.15), (1.3.17), or (1.3.18) the integral representation (6.1.11), becomes

$$u(\mathbf{x}, t) = \frac{1}{2\pi i} \int_{-\infty}^{\infty} e^{z(\zeta)t} \hat{u}(\mathbf{x}, z(\zeta)) \acute{z}(\zeta) d\zeta, \tag{6.1.12}$$

The approximation of (6.1.12) by trapezoidal rule with uniform step size k, and quadrature points $z_j = z(\zeta_j), \zeta_j = jk$, is given as

$$u_k(\mathbf{x}, t) = \frac{k}{2\pi i} \sum_{j=-M}^{M} e^{z_j t} \hat{u}(\mathbf{x}, z_j) \acute{z}_j. \tag{6.1.13}$$

6.2 Numerical problems

The method is applied to the partial integro differential equation to validate our numerical scheme. The multiquadrics $\phi(r, \varepsilon) = (1 + (\varepsilon r)^2)^{1/2}$ are used in all our computations and solution accuracy depends on parameter ε. A number of criterias are available in the literature for choosing optimal values of shape parameters. We use the Uncertainty principal [223] to select the shape parameter for good accuracy.

Problem 6.2.1. *We consider the one dimensional partial integro differential equation [255] to test our method,*

$$u_t(x,s) - \int_0^t \beta(t-s)u_{xx}(x,t)ds- = f(x,t), \quad -1 \leq x \leq 1, \quad t > 0. \tag{6.2.1}$$

where

$$f(x,t) = \frac{3}{2}(1-x^2)t^{\frac{1}{2}} + \frac{3\sqrt{\pi}}{4}t^2$$

and

$$\beta(t) = (\pi t)^{\frac{-1}{2}} \quad for \quad t > 0.$$

The initial and boundary conditions are

$$u(x,0) = 0$$

and

$$u(-1,t) = u(1,t) = 0, \quad t > 0$$

The true solution of the problem is $u(x,t) = t^{\frac{3}{2}}(1-x^2)$. The problem is solved over the domain $-1 \leq x \leq 1$ at $t = 1$. Different quadrature points are used along the parabolic contour C_1 and hyperbolic contour C_3. These points are generated by MATLAB statement $\zeta = -M : k : M$ for parabolic contour C_1, and for hyperbolic contour C_3. The parameters used are $\theta = 0.1, \delta = 0.1541, r = 0.1387, \omega = 2, c = 0.1, t_0 = 0.5$ and $T = 5$. The other optimal parameters are given in (1.3.15) and (1.3.18) for both contours parabolic C_1 and hyperbolic C_3 respectively. The L_∞ error and error estimates for both the contours parabolic and hyperbolic are shown in table 6.1 and 6.2 respectively. Various number of points N in the global domain Ω and n in the local domain Ω_i are used. The shape parameter is optimized using the uncertainty principle [223]. This method give us almost exact solution in time, error occurs only in spatial discretization. So we can approximate partial integro differential equation

very accurately in time without any time instability issue. The local nature of the method make it more attractive for such type of problems.

N	M	n	L_∞ (error)	E_1
20	30	10	3.69e-004	8.01e-010
30	50	12	4.83e-005	6.92e-016
35	70	13	6.62e-005	5.97e-022
50	90	14	8.05e-005	5.15e-028
[255] 8.578e-005				

Table 6.1: Numerical solution for problem 6.2.1 in the domain $[-1, 1]$, $t = 1$, and $1e12 \leq \kappa \leq 1e16$, along the contour C_1

N	M	n	L_∞ (error)	E_3
20	30	10	2.75e-004	0.537
30	50	12	3.80e-005	0.062
35	70	13	6.59e-005	0.007
50	90	14	8.05e-005	8.182e-004
[255] 8.578e-005				

Table 6.2: Numerical solution for problem 6.2.1 in the domain $[-1, 1]$, $t = 1$, and $1e12 \leq \kappa \leq 1e16$, along the contour C_3

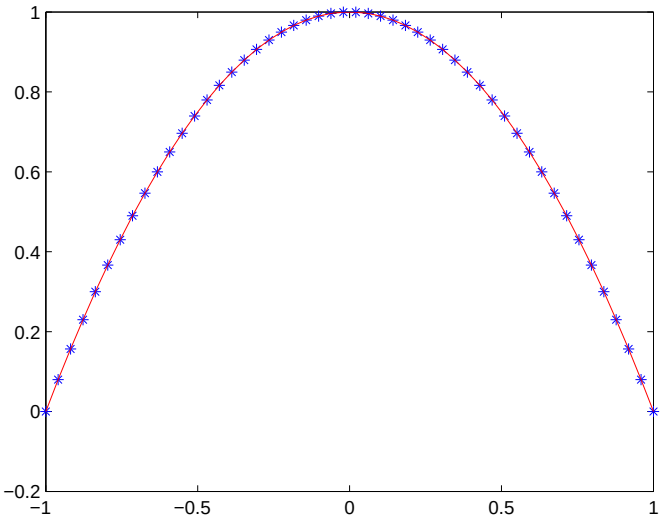

Figure 6.1: Numerical and exact solution corresponding to the problem 6.2.1 over the domain $[-1, 1]$ when $N = 50, n = 10, M = 40$.

Problem 6.2.2. *Next we tested the present method to the two dimensional partial integro-differential equation [255],*

$$u_t(x, y, s) - \int_0^t \beta(t-s)\Delta u(x, y, t)ds = f(x, y, t), \quad x, y \in \Omega \equiv (-1, 1)^2, \quad t > 0. \quad (6.2.2)$$

where

$$f(x, y, t) = \frac{3\sqrt{\pi}}{4}\frac{(1-x^2)(1-y^2)}{z^{\frac{3}{2}}} + \frac{3\sqrt{\pi}}{4}\frac{(4-2x^2-2y^2)}{z^3}$$

and

$$\beta(t) = (\pi t)^{\frac{-1}{2}} \quad for \quad t > 0.$$

The initial and boundary conditions are

$$u(x, y, 0) = 0, x, y \in \Omega,$$

and

$$u(x,y,t) = u(x,y,t) = 0, x, y \in \partial\Omega, \quad t > 0$$

. Here we tested our method for two dimensional PIDE with exact solution $u(x,y,t) = (t^{\frac{3}{2}})(1-x^2)(1-y^2)$ over the domain $[-1,1]^2$ at $t = 1$. Different quadrature points are used along the parabolic contour C_1 and hyperbolic contour C_3.The parameters used are $\theta = 0.1, \delta = 0.1541, r = 0.1387, \omega = 2, c = 0.1, t_0 = 0.5$ and $T = 5$. The other optimal parameters are given in (1.3.15) and (1.3.18) for both contours parabolic C_1 and hyperbolic C_3 respectively. The L_∞ error and error estimates for both the contours parabolic and hyperbolic are shown in table 6.3 and 6.4 respectively. Various number of points N in the global domain Ω and n in the local domain Ω_i are used. The shape parameter is optimized using the uncertainty principle [223]. Similar performance is observed like one we observed in problem 6.2.1. So the proposed method is best for approximating PIDE equation in multi dimensions as well.

N	M	n	L_∞ (error)	E_1
20	30	8	2.85e-004	8.01e-010
25	50	12	1.21e-002	6.92e-016
30	60	13	7.20e-004	6.43e-019
40	70	14	6.31e-004	5.97e-022
[255] 1.679e-004				

Table 6.3: Numerical solution for problem 6.2.2 in the domain $[-1,1]^2$, $t = 1$, and $1e12 \leq \kappa \leq 1e16$, along the contour C_1

N	M	n	L_∞ (error)	E_3
20	30	8	1.10e-003	0.537
25	50	12	1.01e-002	0.062
30	60	13	7.20e-004	0.021
40	70	14	6.31e-004	0.007
[255] 1.679e-004				

Table 6.4: Numerical solution for problem 6.2.2 in the domain $[-1,1]^2$, $t = 1$, and $1e12 \leq \kappa \leq 1e16$, along the contour C_3

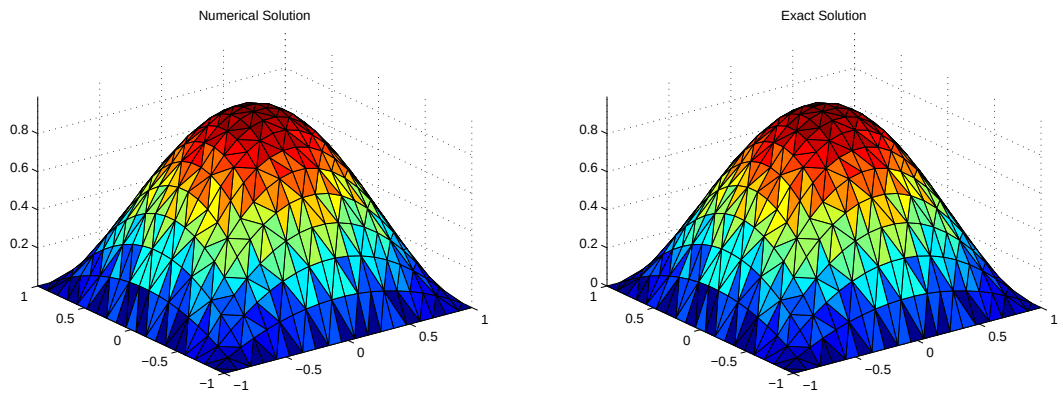

Figure 6.2: Numerical and exact solution corresponding to the problem 6.2.2 over the domain $[-1,1]$ when $N = 20, n = 8, M = 30$.

6.3 Chapter summary

In this chapter, the numerical solution of the partial integro-differential equations is obtained very accurately and efficiently. The method is tested for 1-D and 2-D

problems. The present method recovered the more accurate results as compared to other methods.

Chapter 7

Conclusions

In this thesis the Laplace transform is coupled with the localized radial kernel based method. The method is implemented for computing diffusion problems of fractional orders. The main benefit of the method is to remove the time derivative of fractional order and the reduced time independent PDEs into a system of PDEs without time derivative in the Laplace space. The solution of the resulted PDEs are carried out through localized radial kernel method. The inversion of the Laplace transform is then approximated to recover the solution of the problem through contour integration using trapezoidal rule. The applicability of the proposed method is restricted to linear equations and those forcing terms whose Laplace transform exists. The method is capable to solve time dependent PDEs of integer and fractional order very accurately and efficiently.

However, there are some difficulties to implement method for those problems, where the Laplace transform cannot handle the non-linear terms. The problem of non-linearity can be overcome with a suitable iterative scheme, e.g [225].
An other problem occur, if the forcing term does not have analytically known Laplace

transform, then we have to find an approximation to the forcing terms that has an analytically known Laplace transform. For the approximation of the forcing term include the work [179], where the least squares approximation, Gauss-Laguerre approximation, and the Prony's method can be used.

The method is applied for solving some diffusion problems and partial integro-differential equations of fractional orders very accurately. The proposed method is an alternative for solving such types of fractional order problems whose Laplace transform can be approximated easily. We also discussed the stability and convergence of the method.

Bibliography

[1] J. Isenberg and C. Gutfinger. Heat transfer to a draining film. *International Journal of Heat and Mass Transfer*, 16(2):505–512, 1973.

[2] C. R. Gane and P. L. Stephenson. An explicit numerical method for solving transient combined heat conduction and convection problems. *International Journal for Numerical Methods in Engineering*, 14(8):1141–1163, 1979.

[3] V. Guvanasen and R. E. Volker. Numerical solutions for solute transport in unconfined aquifers. *International Journal for Numerical Methods in Fluids*, 3(2):103–123, 1983.

[4] M. Wang, Y. Zhou, and Z. Li. Application of a homogeneous balance method to exact solutions of nonlinear equations in mathematical physics. *Physics Letters A*, 216(1-5):67–75, 1996.

[5] T. Cecil, J. Qian, and S. Osher. Numerical methods for high dimensional hamilton–jacobi equations using radial basis functions. *Journal of Computational Physics*, 196(1):327–347, 2004.

[6] E. Orsingher and L. Beghin. Time fractional telegraph equations and telegraph processes with Brownian time. *Probability Theory and Related Fields*, 128(1):141–160, 2004.

[7] A. Mohebbi and M. Dehghan. High order compact solution of the one dimensional heat and advection diffusion equations. *Applied Mathematical Modelling*, 34(10):3071–3084, 2010.

[8] M. Dehghan. Finite difference procedures for solving a problem arising in modeling and design of certain optoelectronic devices. *Mathematics and Computers in Simulation*, 71(1):16–30, 2006.

[9] G. Kosec and B. Sarler. Local RBF collocation method for darcy flow. *CMES:Computer Modeling in Engineering and Sciences*, 25(3):197–207, 2008.

[10] R. Gorenflo, F. Mainardi, D. Moretti, G. Pagnini, and P. Paradisi. Discrete random walk models for space-time fractional diffusion. *Chemical Physics*, 284(1):521–541, 2002.

[11] D. del Castillo-Negrete, B. A. Carreras, and V. E. Lynch. Front dynamics in reaction-diffusion systems with levy flights: a fractional diffusion approach. *Physical Review Letters*, 91(1):018302, 2003.

[12] H. Scher and E. W. Montroll. Anomalous transit-time dispersion in amorphous solids. *Physical Review B*, 12(6):2455, 1975.

[13] E. Scalas, R. Gorenflo, and F. Mainardi. Fractional calculus and continuous-time finance. *Physica A: Statistical Mechanics and its Applications*, 284(1):376–384, 2000.

[14] M. D. Marcozzi, S. Choi, and C. S. Chen. On the use of boundary conditions for variational formulations arising in financial mathematics. *Applied Mathematics and Computation*, 124(2):197–214, 2001.

[15] Y. C. Hon. A quasi-radial basis functions method for american options pricing. *Computers and Mathematics with Applications*, 43(3-5):513–524, 2002.

[16] G. E. Fasshauer, A. Q. M. Khaliq, and D. A. Voss. Using meshfree approximation for multi-asset american options. *Journal of the Chinese Institute of Engineers*, 27(4):563–571, 2004.

[17] W. Chen and S. Wang. A power penalty method for a 2D fractional partial differential linear complementarity problem governing two-asset american option pricing. *Applied Mathematics and Computation*, 305:174–187, 2017.

[18] U. Pettersson, E. Larsson, G. Marcusson, and J. Persson. Improved radial basis function methods for multi dimensional option pricing. *Journal of Computational and Applied Mathematics*, 222(1):82–93, 2008.

[19] E. Larsson, K. Åhlander, and A. Hall. Multi-dimensional option pricing using radial basis functions and the generalized fourier transform. *Journal of Computational and Applied Mathematics*, 222(1):175–192, 2008.

[20] R. Company, L. Jódar, and J. R. Pintos. A numerical method for european option pricing with transaction costs nonlinear equation. *Mathematical and Computer Modelling*, 50(5):910–920, 2009.

[21] J. C. Ndogmo and D. B. Ntwiga. High order accurate implicit methods for barrier option pricing. *Applied Mathematics and Computation*, 218(5):2210–2224, 2011.

[22] A. R. A. Anderson and M. A. J Chaplain. Continuous and discrete mathematical models of tumor-induced angiogenesis. *Bulletin of mathematical biology*, 60(5):857–899, 1998.

[23] P. D. Dale, P. K. Maini, and J. A. Sherratt. Mathematical modeling of corneal epithelial wound healing. *Mathematical biosciences*, 124(2):127–147, 1994.

[24] L. Olsen, J. A. Sherratt, P. K. Maini, and F. Arnold. A mathematical model for the capillary endothelial cell-extracellular matrix interactions in wound-healing angiogenesis. *Mathematical Medicine and Biology: A Journal of the IMA*, 14(4):261–281, 1997.

[25] H.D. Jong. Modeling and simulation of genetic regulatory systems: a literature review. *Journal of computational biology*, 9(1):67–103, 2002.

[26] P. K. Maini, D. S. McElwain, and D. Leavesley. Travelling waves in a wound healing assay. *Applied Mathematics Letters*, 17(5):575–580, 2004.

[27] F. Ascione, S. Caserta, and S. Guido. The wound healing assay revisited: A transport phenomena approach. *Chemical Engineering Science*, 160:200–209, 2017.

[28] L. Edelstein-Keshet. *Mathematical models in Biology*. McGraw-Hill, 1988.

[29] J. D. Murray. *Mathematical Biology-I: an introduction Interdisciplinary Applied Mathematics V. 17*. Springer-Verlag New York Incorporated, 2002.

[30] J. D. Murray. *Mathematical Biology-II Spatial Models and Biomedical Applications Interdisciplinary Applied Mathematics V. 18*. Springer-Verlag New York Incorporated, 2002.

[31] M. Caputo. Elasticitá e dissipazione (elasticity and anelastic dissipation). *Zanichelli, Bologna*, 1969.

[32] P. J. Torvik and R. L. Bagley. On the appearance of the fractional derivative in the behavior of real materials. *Journal of Applied Mechanics*, 51(2):294–298, 1984.

[33] E. Scalas, R. Gorenflo, and F. Mainardi. Uncoupled continuous-time random walks: Solution and limiting behavior of the master equation. *Physical Review E*, 69(1):011107, 2004.

[34] R. Marks and M. Hall. Differintegral interpolation from a bandlimited signal's samples. *IEEE Transactions on Acoustics, Speech, and Signal Processing*, 29(4):872–877, 1981.

[35] K. Diethelm and A. D. Freed. On the solution of nonlinear fractional-order differential equations used in the modeling of viscoplasticity. In *Scientific Computing in Chemical Engineering II*, pages 217–224. Springer, 1999.

[36] A. Freed, K. Diethelm, and Y. Luchko. Fractional-order viscoelasticity (fov): Constitutive development using the fractional calculus: First annual report. 2002.

[37] I. Podlubny. *Fractional differential equations: an introduction to fractional derivatives, fractional differential equations, to methods of their solution and some of their applications*, volume 198. Academic press, 1998.

[38] K. B. Oldham and J. Spanier. *The fractional calculus theory and applications of differentiation and integration to arbitrary order*, volume 111. Academic Press, New York, London, 1974.

[39] R. L. Bagley and P. J. Torvik. A theoretical basis for the application of fractional calculus to viscoelasticity. *Journal of Rheology*, 27(3):201–210, 1983.

[40] R. Metzler and J. Klafter. The restaurant at the end of the random walk: recent developments in the description of anomalous transport by fractional dynamics. *Journal of Physics A: Mathematical and General*, 37(31):R161, 2004.

[41] G. D. Smith. *Numerical solution of partial differential equations: finite difference methods*. Second edition, Oxford University Press, 1978.

[42] A. J. Davies. *The finite element method: a first approach*. Oxford University Press, 1985.

[43] R. J. LeVeque. *Finite volume methods for hyperbolic problems (Vol.31)*. Cambridge university press, 2002.

[44] C. A. Brebbia and J. Dominguez. *Boundary elements, an introductory course*. McGraw-Hill/Computational Mechanics Publications., 1989.

[45] G. E. Fasshauer. *Meshfree Approximation Methods with Matlab:(With CD-ROM). Vol. 6.* World Scientific Publishers Co Inc, Singapore, 2007.

[46] A. J. M. Ferreira, E. J. Kansa, G. E. Fasshauer, and V. M. A. Leitão. *Progress on meshless methods*. Springer, 2009.

[47] G. E. Fasshauer and M. McCourt. *Kernel-based approximation methods using Matlab*. World Scientific, 2016.

[48] P. Zhuang, Y. T. Gu, F. Liu, I. Turner, and P. K. D. V. Yarlagadda. Time dependent fractional advection diffusion equations by an implicit MLS meshless method. *International Journal for Numerical Methods in Engineering*, 88(13):1346–1362, 2011.

[49] A. Shirzadi, L. Ling, and S. Abbasbandy. Meshless simulations of the two dimensional fractional time convection diffusion reaction equations. *Engineering Analysis with Boundary Elements*, 36(11):1522–1527, 2012.

[50] M. Ramezani, M. Mojtabaei, and D. Mirzaei. DMLPG solution of the fractional advection diffusion problem. *Engineering Analysis with Boundary Elements*, 59:36–42, 2015.

[51] W. Chen, L. Ye, and H. Sun. Fractional diffusion equations by the Kansa method. *Computers and Mathematics with Applications*, 59(5):1614–1620, 2010.

[52] Y. T. Gu and G. R. Liu. A local point interpolation method for static and dynamic analysis of thin beams. *Computer Methods in Applied Mechanics and Engineering*, 190(42):5515–5528, 2001.

[53] W. Chen. Symmetric boundary knot method. *Engineering Analysis with Boundary Elements*, 26(6):489–494, 2002.

[54] Z. Fu, W. Chen, and C. Zhang. Boundary particle method for cauchy inhomogeneous potential problems. *Inverse problems in Science and Engineering*, 20(2):189–207, 2012.

[55] W. Chen, L. J. Shen, Z. J. Shen, and G. W. Yuan. Boundary knot method for poisson equations. *Engineering Analysis with Boundary Elements*, 29(8):756–760, 2005.

[56] B. Jin and Y. Zheng. Boundary knot method for the cauchy problem associated with the inhomogeneous helmholtz equation. *Engineering Analysis with Boundary Elements*, 29(10):925–935, 2005.

[57] W. Chen. Singular boundary method: a novel, simple, meshfree, boundary collocation numerical method. *Chinese Journal of Solid Mechanics*, 30(6):592–599, 2009.

[58] G. Yan, W. Chen, and C. Z. Zhang. Singular boundary method for solving plane strain elastostatic problems. *International Journal of Solids and Structures*, 48(18):2549–2556, 2011.

[59] D. L. Young, K. H. Chen, and C. L. Lee. Novel meshless method for solving the potential problems with arbitrary domain. *Journal of Computational Physics*, 209(1):290–321, 2005.

[60] T. Belytschko, Y. Y. Lu, and L. Gu. Element free galerkin methods. *International Journal for Numerical Methods in Engineering*, 37(2):229–256, 1994.

[61] B. Nayroles, G. Touzot, and P. Villon. Generalizing the finite element method: diffuse approximation and diffuse elements. *Computational mechanics*, 10(5):307–318, 1992.

[62] M. Amirfakhrian, M. Arghand, and E. J. Kansa. A new approximate method for an inverse time dependent heat source problem using fundamental solutions and RBFs. *Engineering Analysis with Boundary Elements*, 64:278–289, 2016.

[63] C. S. Chen, C. M. Fan, and P. H. Wen. The method of approximate particular solutions for solving certain partial differential equations. *Numerical Methods for Partial Differential Equations*, 28(2):506–522, 2012.

[64] G. Yao, B. Sarler, and C. S. Chen. A comparison of three explicit local meshless methods using radial basis functions. *Engineering Analysis with boundary elements*, 35(3):600–609, 2011.

[65] R. Hardy. Multiquadric equations of topography and other irregular surfaces. *Journal of geophysical research*, 76(8):1905–1915, 1971.

[66] J. Duchon. Splines minimizing rotation-invariant semi norms in Sobolev spaces, in constructive theory of functions of several variables. *Constructive theory of functions of several variables*, pages 85–100, 1977.

[67] R. Franke. A critical comparison of some methods for the interpolation of scattered data. *Technical Report NPS-53-79-03, Naval Postgraduate School*, 1979.

[68] R. Franke. Scattered data interpolation: Tests of some methods. *Mathematics of Computation*, 38(157):181–200, 1982.

[69] C. Micchelli. Interpolation of scattered data: Distance matrices and conditionally positive definite functions.II. *Constructive Approximation*, 2(1):11–22, 1986.

[70] E. J. Kansa. Multiquadrics: A scattered data approximation scheme with applications to computational fluid-dynamics$-I$ surface approximations and

partial derivative estimates. *Computers and Mathematics with Applications*, 19(8–9):127–145, 1990.

[71] E. J. Kansa. Multiquadrics: A scattered data approximation scheme with applications to computational fluid-dynamics$-II$ solutions to parabolic, hyperbolic and elliptic partial differential equations. *Computers and Mathematics with Applications*, 19(8):147–161, 1990.

[72] M. A. Golberg, C. S. Chen, and S. R. Karur. Improved multiquadric approximation for partial differential equations. *Engineering Analysis with boundary elements*, 18(1):9–17, 1996.

[73] D. Nardini and C. A. Brebbia. A new approach to free vibration analysis using boundary elements. *Applied mathematical modelling*, 7(3):157–162, 1983.

[74] J. G. Wang and G. R. Liu. On the optimal shape parameters of radial basis function used for 2-D meshless methods. *Computer methods in applied mechanics and engineering*, 191(23–24):2611–2630, 2002.

[75] H. Ding, C. Shu, and D. B. Tang. Error estimates of local multiquadric-based differential quadrature (LMQDQ) method through numerical experiments. *International Journal for Numerical Methods in Engineering*, 63(11):1513–1529, 2005.

[76] C. S. Huang, C. F. Lee, and A. H. D. Cheng. Error estimate, optimal shape factor, and high precision computation of multiquadric collocation method. *Engineering Analysis with Boundary Elements*, 31(7):614–623, 2007.

[77] C. M. C. Roque and A. J. M. Ferreira. Numerical experiments on optimal shape parameters for radial basis function. *Numerical methods for partial differential equations*, 26(3):675–689, 2010.

[78] B. Fornberg and C. Piret. On choosing a radial basis function and a shape parameter when solving a convective PDE on a sphere. *Journal of Computational Physics*, 277(5):2758–2780, 2008.

[79] G. E. Fasshauer and M. J. McCourt. Stable evaluation of gaussian radial basis function interpolants. *SIAM Journal of Scientic Computing*, 34(2):737–762, 2012.

[80] W. R. Madych and S. A. Nelson. Multivariate interpolation and conditionally positive definite functions. *Journal of Approximation Theory*, 4:77–89, 1988.

[81] W. R. Madych and S. A. Nelson. Multivariate interpolation and conditionally positive definite functions-II. *Mathematics of Computation*, 54(189):211–230, 1990.

[82] W. R. Madych and S. A. Nelson. Bounds on multivariate interpolation and exponential error estimates for multiquadric interpolation. *Journal of Approximation Theory*, 70(1):94–114, 1992.

[83] A. H. D. Cheng. Multiquadric and its shape parameter-A numerical investigation of error estimate, condition number, and round off error by arbitrary precision computation. *Engineering Analysis Boundary Elements*, 36(2):220–239, 2012.

[84] Z. M. Wu and R. S. Schaback. Local error estimates for radial basis function interpolation of scattered data. *IMA journal of Numerical Analysis*, 13(1):13–27, 1993.

[85] H. Wendland. *Scattered data approximation. Vol. 17.* Cambridge university press, Cambridge, 2004.

[86] M. D. Buhmann. Multivariate interpolation in Odd dimensional Euclidean space using multiquadrics. *Constructive Approximation*, 6(1):21–34, 1990.

[87] M. D. Buhmann. Multivariate cardinal interpolation with radial basis functions. *Constructive Approximation*, 6(3):225–255, 1990.

[88] R. Schaback. Convergence of unsymmetric kernels-based meshless collocation methods. *SIAM Journal on Numerical Analysis*, 45(1):333–351, 2007.

[89] E. J. Kansa. A strictly conservative spatial approximation scheme for the governing engineering and physics equations over irregular regions and inhomogeneous scattered nodes. *Computers and Mathematics with Applications*, 24(5–6):169–190, 1992.

[90] G. J. Moridis and E. J. Kansa. The Laplace transform multiquadric method: A Highly Accurate Scheme for the Numerical Solution of Partial Differential Equations. *Journal of Applied Science and Computations*, 1993.

[91] M. A. Golberg and C. S. Chen. A bibliography on radial basis function approximation. *Boundary Elements Communications*, 7:155–163, 1996.

[92] M. R. Dubal. Construction of three dimensional black hole initial data via multiquadrics. *Physical Review D*, 45(4):1178–1187, 1992.

[93] M. R. Dubal. Domain decomposition and local refinement for multiquadric approximationsI: Second-order equations in one-dimension. *Journal of Applied Science and Computation*, 1(1):146–171, 1994.

[94] J. R. Xaio and M. A. McCarthy. A local Heaviside weighted meshless method for two-dimensional solids using radial basis functions. *Computational Mechanics*, 31(3):301–315, 2003.

[95] C. Franke and R. Schaback. Convergence order estimates of meshless collocation methods using radial basis functions. *Advances in Computational Mathematics*, 8(4):381–399, 1998.

[96] C. Franke and R. Schaback. Solving partial differential equations by collocation using radial basis functions. *Applied Mathematics and Computation*, 93(1):73–82, 1998.

[97] T. Belytschko, Y. Krongauz, D. Organ, M. Fleming, and P Krysl. Meshless method: an overview and recent development. *Computer methods in applied mechanics and engineering*, 139(1–4):3–47, 1996.

[98] W. K. Liu, Y. Chen, S. Jun, J. S. Chen, T. Belytschko, C. Pan, R. A. Uras, and C. T. Chang. Overview and applications of the reproducing kernel particle methods. *Archives of Computational Methods in Engineering*, 3(1):3–80, 1996.

[99] G. E. Fasshauer. Solving partial differential equations by collocation with radial basis functions, in surface fitting and multiresolution methods. *Proceedings of Chamonix. Vol. 1997. Vanderbilt University Press Nashville, TN*, pages 1–8, 1996.

[100] L. Ling and E. J. Kansa. Preconditioning for radial basis functions with domain decomposition methods. *Mathematical and Computer modelling*, 40(13):1413–1427, 2004.

[101] L. Ling and E. J. Kansa. A least squeres preconditioner for radial basis functions collocation methods. *Advances in Computational Mathematics*, 23(1):31–54, 2005.

[102] Y. C. Hon, K. F. Cheung, X. Z. Mao, and E. J. Kansa. Multiquadric solution for shallow water equations. *Journal of Hydraulic Engineering*, 125(5):524–533, 1999.

[103] Y. C. Hon and X. Z. Mao. A radial basis function method for solving options pricing model. *Journal of Financial Engineering*, 8:31–50, 1999.

[104] D. L. Young, S. C. Jane, C. Y. Lin, C. L. Chiu, and K. C. Chen. Solution of 2D and 3D Stokes laws using multiquadrics method. *Engineering Analysis with Boundary Elements*, 28(10):1233–1243, 2004.

[105] J. Li, Y. Chen, and D. Pepper. Radial basis function method for 1-D and 2-D groundwater contaminant transport modeling. *Computational Mechanics*, 32(1):10–15, 2003.

[106] B. Šarler, G. Kosec, A. Lorbicka, and R. Vertnik. A meshless approach in solution of multiscale solidification modeling. *Materials Science Forum*, 649:211–216, 2010.

[107] F. F. Dou and Y. C. Hon. Numerical computation for backward time fractional diffusion equation. *Engineering Analysis with Boundary Elements*, 40:138–146, 2014.

[108] E. Larsson and B. Fornberg. A numerical study of some radial basis functions based solution methods for elliptic PDEs. *Computers and Mathematics with Applications*, 46(5):891–902, 2003.

[109] M. D. Buhmann. *Radial basis functions: theory and implementations (Vol.12)*. Cambridge University Press, 2003.

[110] G. R. Liu. *Mesh free methods: moving beyond the finite element method*. CRC press, 2002.

[111] S. Islam, S. Haq, and M. Uddin. A meshfree interpolation method for the numerical solution of the coupled nonlinear partial differential equations. *Engineering Analysis with Boundary Elements*, 33(3):399–409, 2009.

[112] H. Wendland. Piecewise polynomial, positive definite and compactly supported radial functions of minimal degree. *Advances in computational Mathematics*, 4(1):389–396, 1995.

[113] Z. Wu. Compactly supported positive definite radial functions. *Advances in Computational Mathematics*, 4(1):283–292, 1995.

[114] G. E. Fasshauer. Solving partial differential equations with radial basis functions: multilevel methods and smoothing. *Advances in Computational Mathematics*, 11(2–3):139–159, 1999.

[115] X. Zhou, Y. C. Hon, and J. Li. Overlapping domain decomposition method by radial basis functions. *Applied Numerical Mathematics*, 44(1–2):241–255, 2003.

[116] E. J. Kansa and Y. C. Hon. Circumventing the ill conditioning problem with multiquadric radial basis functions: applications to elliptic partial differential equations. *Computers and Mathematics with applications*, 39(7–6):123–137, 2000.

[117] Y. C. Hon, R. Schaback, and X. Zhou. An adaptive greedy algorithm for solving large RBF collocation problems. *Numerical Algorithms*, 32(1):13–25, 2003.

[118] B. Šarler and R. Vertnik. Meshfree explicit local radial basis function collocation method for diffusion problems. *Computers and Mthematics with Applications*, 51(8):1269–1282, 2006.

[119] C. Shu, H. Ding, and K. S. Yeo. Local radial basis function-based differential quadrature method and its application to solve two dimensional in compressible Navier's Stokes equations. *Computer Methods in Applied Mechanics and Engineering*, 192(7):941–954, 2003.

[120] B. Šarler and R. Vertnik. Meshless local radial basis function collocation method for convective–diffusive solid-liquid phase change problems. *International Journal of Numerical Methods for Heat and Fluid Flow*, 16(5):617–640, 2006.

[121] R. Vertnik, M. Založnik, and B. Šarler. Solution of transient direct-chill aluminium billet casting problem with simultaneous material and interphase moving boundaries by a meshless method. *Engineering Analysis with Boundary Elements*, 30(10):847–855, 2006.

[122] I. Kovačević and B. Šarler. Solution of a phase-field model for dissolution of primary particles in binary aluminum alloys by an r–adaptive meshfree method. *Materials Science and Engineering*, 51(8):423–428, 2005.

[123] B. Šarler. A radial basis function collocation approach in computational fluid dynamics. *Computer Modelling in Engineering and Sciences*, 7(2):185–193, 2005.

[124] E. Divo and A. J. Kassab. An efficient localized rbf meshless method applied to fluid flow and conjugate heat transfer. *ASME Paper IMECE2005-82150*, pages 241–250, 2005.

[125] R. Vertnik and B. Šarler B. Solution of incompressible turbulent flow by a mesh-free method. *CMES:Computer Modeling in Engineering and Sciences*, 44(1):65–96, 2009.

[126] M. Uddin, A. Ali, Kamran, M. Imran, and Z. Minullah. Simulation of diffusion equation in irregular domain using local kernel-based method. *Journal of Applied Environmental and Biological Sciences*, 4(7S):428–435, 2014.

[127] M. Uddin, H. ALi, and A. Ali. Kernel based local meshless method for solving multi dimensional wave equations in irregular domain. *CMES: Computer Modeling in Engineering and Sciences*, 107(6):463–479, 2015.

[128] S. Wei, W. Chen, and Y. C. Hon. Implicit local radial basis function method for solving two dimensional time fractional diffusion equations. *Thermal Science*, 19(1):59–67, 2015.

[129] Y. C. Hon, B. Šarler, and D.F. Yun. Local radial basis function collocation method for solving thermo-driven fluid-flow problems with free surface. *Engineering Analysis with Boundary Elements*, 57(1):2–8, 2015.

[130] D. F. Yun and Y. C. Hon. Improved localized radial basis function collocation method for multi dimensional convection dominated problems. *Engineering Analysis with Boundary Elements*, 67:63–80, 2016.

[131] F. J. Rizzo and D. J. Shippy. A method of solution for certain problems of transient heat conduction. *AIAA J.*, 8(11):2004–2009, 1968.

[132] R. de. Prony. Essai éxperimental et analytique: sur les lois de la dilatabilité de fluides élastique et sur celles de la force expansive de la vapeur de lalkool, á différentes températures. *J. lÉcole. Polytech*, 1:24–76, 1795.

[133] D. W. Kammler. Prony's method for completely monotonic functions. *Journal of Mathematical Analysis and Applications*, 57(3):560–570, 1977.

[134] H. Dubner and J. Abate. Numerical inversion of laplace transforms by relating them to the finite fourier cosine transform. *Journal of the ACM (JACM)*, 15(1):115–123, 1968.

[135] F. Durbin. Numerical inversion of laplace transforms: an efficient improvement to dubner and abate's method. *The Computer Journal*, 17(4):371–376, 1974.

[136] R. M. Simon, M. T. Stroot, and G. H. Weiss. Numerical inversion of Laplace transforms with application to percentage labeled mitoses experiments. *Computers and Biomedical Research*, 5(6):596–607, 1972.

[137] F. Veillon. *Quelques nouvelles méthodes pour le calcul numérique de la transformée inverse de Laplace*. PhD thesis, Université Joseph-Fourier-Grenoble I, 1972.

[138] K. S. Crump. Numerical inversion of laplace transforms using a fourier series approximation. *Journal of the ACM (JACM)*, 23(1):89–96, 1976.

[139] A. F. Moench and A. Ogata. A numerical inversion of the Laplace transform solution to radial dispersion in a porous medium. *Water Resources Research*, 17(1):250–252, 1981.

[140] C. S. Chen. Analytical and approximate solutions to radial dispersion from an injection well to a geological unit with simultaneous diffusion into adjacent strata. *Water Resources Research*, 21(8):1069–1076, 1985.

[141] C. S. Chen. Solutions for radionuclide transport from an injection well into a single fracture in a porous formation. *Water resources research*, 22(4):508–518, 1986.

[142] H. Stehfest. Algorithm 368: Numerical inversion of laplace transforms [d5]. *Communications of the ACM*, 13(1):47–49, 1970.

[143] H. Stehfest. Remark on algorithm 368: Numerical inversion of laplace transforms. *Communications of the ACM*, 13(10):624, 1970.

[144] C. S. Chen. Solutions approximating solute transport in a leaky aquifer receiving wastewater injection. *Water Resources Research*, 25(1):61–72, 1989.

[145] C. S. Chen. Semianalytical Solutions for Radial Dispersion in a Three-Layer Leaky Aquifer System. *Groundwater*, 29(5):663–670, 1991.

[146] Y. J. Chen, H. D. Yeh, and K. J. Chang. A mathematical solution and analysis of contaminant transport in a radial two-zone confined aquifer. *Journal of contaminant hydrology*, 138(2):75–82, 2012.

[147] C. T. Liu, H. D. Yeh, and L. M. Yeh. Modeling contaminant transport in a two-aquifer system with an intervening aquitard. *Journal of hydrology*, 499:200–209, 2013.

[148] F. R. De Hoog, J. H. Knight, and A. N. Stokes. An improved method for numerical inversion of laplace transforms. *SIAM Journal on Scientific and Statistical Computing*, 3(3):357–366, 1982.

[149] J. S. Chen, C. W. Liu, and C. M. Liao. Two-dimensional Laplace-transformed power series solution for solute transport in a radially convergent flow field. *Advances in Water Resources*, 26(10):1113–1124, 2003.

[150] A. F. Moench. Convergent radial dispersion: a note on evaluation of the Laplace transform solution. *Water resources research*, 27(12):3261–3264, 1991.

[151] A. F. Moench. Convergent radial dispersion: A Laplace transform solution for aquifer tracer testing. *Water Resources Research*, 25(3):439–447, 1989.

[152] A. Talbot. The accurate numerical inversion of Laplace transform. *IMA Journal of Applied Mathematics*, 23(1):97–120, 1979.

[153] M. Rizzardi. A modification of Talbot's method for the simultaneous approximation of several values of the inverse Laplace transform. *ACM Transactions on Mathematical Software (TOMS)*, 21(4):347–371, 1995.

[154] D. P. Bullivant and M. J. O'sullivan. Matching a field tracer test with some simple models. *Water Resources Research*, 25(8):1879–1891, 1989.

[155] H. Zhan, Z. Wen, and G. Gao. An analytical solution of two-dimensional reactive solute transport in an aquifer-aquitard system. *Water resources research*, 45(10):592–599, 2009.

[156] F. J. Leij, M. T. van Genuchten, and J. H. Dane. Mathematical analysis of one-dimensional solute transport in a layered soil profile. *Soil Science Society of America Journal*, 55(4):944–953, 1991.

[157] F. Cornaton and P. Perrochet. Groundwater age, life expectancy and transit time distributions in advectivedispersive systems: 1. Generalized reservoir theory. *Advances in Water Resources*, 29(9):1267–1291, 2006.

[158] W. T. Weeks. Numerical inversion of Laplace transforms using Laguerre functions. *Journal of the ACM (JACM)*, 13(3):419–429, 1966.

[159] R. C. Schwartz, K. J. McInnes, A. S. Juo, L. P. Wilding, and D. L. Reddell. Boundary effects on solute transport in finite soil columns. *Water resources research*, 35(3):671–681, 1999.

[160] F. J. Leij and M. T. Van Genuchten. Approximate analytical solutions for solute transport in two-layer porous media. *Transport in Porous Media*, 18(1):65–85, 1995.

[161] G. Gao, H. Zhan, S. Feng, B. Fu, Y. Ma, and G. Huang. A new mobile-immobile model for reactive solute transport with scale-dependent dispersion. *Water Resources Research*, 46(8):1–16, 2010.

[162] E. L. Post. Generalized differentiation. *Transactions of the American Mathematical Society*, 32(4):723–781, 1930.

[163] P. O. Kano and M. Brio. Application of post's formula to optical pulse propagation in dispersive media. *Computers and mathematics with applications*, 59(2):629–650, 2010.

[164] A. Papoulis. A new method of inversion of the Laplace transform. *Quarterly of Applied Mathematics*, 14(4):405–414, 1957.

[165] R. A. Schapery. Approximate methods of transform inversion for viscoelastic stress analysis. *In: Proceedings of the 4th US national congress applied mechanics, New York*, 1962.

[166] T. L. Cost. Approximate Laplace transform inversions in viscoelastic stress analysis. *AIAA J*, 2(12):2157–2166, 1964.

[167] V. Zakian. Numerical inversion of laplace transforms. *Electronics Letters*, 5(6):120–121, 1969.

[168] R. Piessens. Gaussian quadrature formulas for the numerical integration of Bromwich's integral and the inversion of the Laplace transform. *Journal of Engineering Mathematics*, 5(1):1–9, 1971.

[169] R. Piessens and N. D. P. Dang. A bibliography on numerical inversion of the Laplace transform and applications : A Supplement. *Journal of Computational and Applied Mathematics*, 2(3):225–228, 1976.

[170] G. J. Moridis and D. L. Reddell. The Laplace transform finite difference method for simulation of flow through porous media. *Water Resources Research*, 27(8):1873–1884, 1991.

[171] G. J. Moridis, D. A. McVay, D. L. Reddell, and T. A. Blasingame. The Laplace transform finite difference (ltfd) numerical method for the simulation of compressible liquid flow in reservoirs. *SPE Advanced Technology Series*, 2(02):122–131, 1994.

[172] G. J. Moridis and D. L. Reddell. The Laplace transform finite element (LTFE) numerical method for the solution of the ground water equation. *presented at the 1991 AGU Spring Meeting, Baltimore, May 28-June 1, 1991, EOS Trans. of the AGU*, 72(17):223–, 1991.

[173] G. J. Moridis and D. L. Reddell. The Laplace transform boundary element (ltbe) method for the solution of diffusion-type equations. *Boundary Elements XIII. Springer, Dordrecht*, pages 83–97, 1991.

[174] D. Crann, J. A. Davies, and J. Mushtaq. Parallel laplace transform boundary element methods for diffusion problems. *WIT Transactions on Modelling and Simulation*, 21, 1998.

[175] E. A. Sudicky and R. G. McLaren. The Laplace transform Galerkin technique for large-scale simulation of mass transport in discretely fractured porous formations. *Water Resources Research*, 28(2):499–514, 1992.

[176] Z. J. Fu, W. Chen, and H. T. Yang. Boundary particle method for Laplace transformed time fractional diffusion equations. *Journal of Computational Physics*, 235:52–66, 2013.

[177] Q. T. L. Gia and W. Mclean. Solving the heat equation on the unit sphere via Laplace transforms and radial basis functions. *Advances in Computational Mathematics*, 40(2):353–375, 2014.

[178] D. Sheen, I. H. Sloan, and V. Thomée. A parallel method for time-discretization of parabolic problems based on contour integral representation and quadrature. *Mathematics of Computation of the American Mathematical Society*, 69(229):177–195, 2000.

[179] D. Sheen, I. H. Slaon, and V. Thomée. A parallel method for time discretization of parabolic equations based on Laplace transformation and quadrature. *IMA Journal of Numerical Analysis*, 23(2):269–299, 2003.

[180] W. McLean and V. Thomee. Time discretization of an evolution equation via Laplace transforms. *IMA Journal of Numerical Analysis*, 24(3):439–463, 2004.

[181] W. McLean and V. Thomee. Numerical solution via Laplace transforms of a fractional order evolution equation. *Journal of Integral Equations and Applications*, 22(1):57–94, 2010.

[182] M. L. Fernandez and C. Palencia. On the numerical inversion of the Laplace transform of certain holomorphic mappings. *Applied Numerical Mathematics*, 51(2–3):289–303, 2004.

[183] M. L. Fernández, C. Palencia, and A. Schädle. A spectral order method for inverting sectorial laplace transforms. *SIAM journal on numerical analysis*, 44(3):1332–1350, 2006.

[184] J. A. C. Weideman. Optimizing Talbots contours for the inversion of the Laplace transform. *SIAM Journal on Numerical Analysis*, 44(6):2342–2362, 2006.

[185] J. A. C. Weideman and L. N. Trefethen. Parabolic and hyperbolic contours for computing the Bromwich integral. *Mathematics of Computation*, 76(259):1341–1356, 2007.

[186] R. Schaback. *"Kernel-based meshless methods".Lecture Notes for Taught Course in Approximation Theory.* Georg-August-Universitt Gttingen, 2007.

[187] A. Murli and M. Rizzardi. Algorithm 682: Talbot's method of the laplace inversion problems. *ACM Transactions on Mathematical Software (TOMS)*, 16(2):158–168, 1990.

[188] B. Dingfelder and J. A. C. Weideman. An improved talbot method for numerical laplace transform inversion. *Numerical Algorithms*, 68(1):167–183, 2015.

[189] R. Du, W. R. Cao, and Z. Z. Sun. A compact difference scheme for the fractional diffusion-wave equation. *Applied Mathematical Modelling*, 34(10):2998–3007, 2010.

[190] K. S. Miller and B. Ross. An introduction to the fractional calculus and fractional differential equations. 1993.

[191] E. Orsingher and X. Zhao. The space fractional telegraph equation and the related fractional telegraph process. *Chinese Annals of Mathematics*, 24(1):45–56, 2003.

[192] Y. Z. Povstenko. Fractional heat conduction equation and associated thermal stress. *Journal of Thermal stresses*, 28(1):83–102, 2004.

[193] C. Tadjeran and M. M. Meerschaert. A second order accurate numerical method for the two dimensional fractional diffusion equation. *Journal of Computational Physics*, 220(2):813–823, 2007.

[194] A. Saadatmandi, M. Dehghan, and M. R. Azizi. The Sinc–Legendre collocation method for a class of fractional convection–diffusion equations with variable coefficients. *Communications in Nonlinear Science and Numerical Simulation*, 17(11):4125–4136, 2012.

[195] K. Diethelm and N. J. Ford. Analysis of fractional differential equations. *Journal of Mathematical Analysis and Applications*, 265(2):229–248, 2002.

[196] W. Wyss. The fractional diffusion equation. *Journal of Mathematical Physics*, 27(11):2782–2785, 1986.

[197] T. A. M. Langlands and B. I. Henry. The accuracy and stability of an implicit solution method for the fractional diffusion equation. *Journal of Computational Physics*, 205(2):719–736, 2005.

[198] Z. Z. Sun and X. Wu. A fully discrete difference scheme for a diffusion-wave system. *Applied Numerical Mathematics*, 56(2):193–209, 2006.

[199] S.Chen, F. Liu, P. Zhuang, and V. Anh. Finite difference approximations for the fractional fokker–planck equation. *Applied Mathematical Modelling*, 33(1):256–273, 2009.

[200] M. Cui. Compact finite difference method for the fractional diffusion equation. *Journal of Computational Physics*, 228(20):7792–7804, 2009.

[201] S. Esmaeili and M. Shamsi. A pseudo-spectral scheme for the approximate solution of a family of fractional differential equations. *Communications in Nonlinear Science and Numerical Simulation*, 16(9):3646–3654, 2011.

[202] C. M. Chen, F. Liu, I. Turner, and V. Anh. Numerical methods with fourth-order spatial accuracy for variable-order nonlinear stokes first problem for a heated generalized second grade fluid. *Computers & Mathematics with Applications*, 62(3):971–986, 2011.

[203] S. Momani. Analytic and approximate solutions of the space and time fractional telegraph equations. *Applied Mathematics and Computation*, 170(2):1126–1134, 2005.

[204] S. Momani, Z. Odibat, and A. Alawneh. Variational iteration method for solving the space and time fractional KdV equation. *Numerical Methods for Partial Differential Equations*, 24(1):262–271, 2008.

[205] M. Dehghan, S. A. Yousefi, and A. Lotfi. The use of He's variational iteration method for solving the telegraph and fractional telegraph equations. *International Journal for Numerical Methods in Biomedical Engineering*, 27(2):219–231, 2011.

[206] D. A. Murio. Implicit finite difference approximation for time fractional diffusion equations. *Computer and Mathematics with Applications*, 56:1138–1145, 2008.

[207] K. Moaddy, S. Momani, and I. Hashim. The non standard finite difference scheme for linear fractional PDEs in fluid mechanics. *Computers and Mathematics with Applications*, 61(4):1209–1216, 2011.

[208] A. Mohebbi, M. Abbaszadeh, and M. Dehghan. A high order and unconditionally stable scheme for the modified anomalous fractional sub diffusion equation with a nonlinear source term. *Journal of Computational Physics*, 240:36–48, 2013.

[209] S. Das, K. Vishal, P. K. Gupta, and A. Yildirim. An approximate analytical solution of time fractional telegraph equation. *Applied Mathematics and Computation*, 217(18):7405–7411, 2011.

[210] M. Dehghan, J. Manafian, and A. Saadatmandi. The solution of the linear fractional partial differential equations using the homotopy analysis method. *Zeitschrift fr Naturforschung-A*, 65(11):935–945, 2010.

[211] G. J. Fix and J. P. Roof. Least squares finite-element solution of a fractional order two-point boundary value problem. *Computers and Mathematics with Applications*, 48(7):1017–1033, 2004.

[212] Y. Jiang and J. Ma. High-order finite element methods for time-fractional partial differential equations. *Journal of Computational and Applied Mathematics*, 235(11):3285–3290, 2011.

[213] H. Brunner, L. Ling, and M. Yamamoto. Numerical simulations of 2d fractional subdiffusion problems. *Journal of Computational Physics*, 229(18):6613–6622, 2010.

[214] Q. Liu, Y. T. Gu, P. Zhuang, F. Liu, and Y. F. Nie. An implicit rbf meshless approach for time fractional diffusion equations. *Computational Mechanics*, 48(1):1–12, 2011.

[215] M. Uddin and S. Haq. RBFs approximation method for time fractional partial differential equations. *Communications in Nonlinear Science and Numerical Simulation*, 16(11):4208–42014, 2011.

[216] R. E. Carlson and T. A. Foley. The parameter r^2 in multiquadric interpolation. *Computers and Mathematics with Applications*, 21(9):29–42, 1991.

[217] T. A. Foley. Near optimal parameter selection for multiquadric interpolation. *Manuscript, Computer Science and Engineering Department, Arizona State University, Tempe*, 1994.

[218] S. Rippa. An algoritham for selecting a good value for the parameter c in radial basis function interpolation. *Advances in Computational Mathematics*, 11(2):193–210, 1999.

[219] C. J. Trahan and R. E. Wyatt. Radial basis function interpolation in the quantum trajectory method: Optimization of the multiquadric shape parameter. *Journal of Computational Physics*, 185(1):27–49, 2003.

[220] G. E. Fasshauer and J. G. Zhang. On choosing optimal shape parameters for RBF approximation. *Numerical Algorithms*, 45(1):345–368, 2007.

[221] M. Scheuerer. An alternative procedure for selecting a good value for the parameter c in RBF interpolation. *Advances in Computational Mathematics*, 34(1):105–126, 2011.

[222] M. Uddin. On the selection of a good value of shape parameter in solving time dependent partial differential equations using RBF approximation method. *Applied Mathematical Modelling*, 38(1):135–144, 2014.

[223] R. Schaback. Error estimates and condition numbers for radial basis function interpolation. *Advances in Computational Mathematics*, 3(3):251–264, 1995.

[224] R. Schaback. Error analysis of nodal meshless methods. In *Meshfree Methods for Partial Differential Equations VIII*, pages 117–143. Springer, 2017.

[225] D. Crann. The laplace transform boundary element method for diffusion-type problems. 2005.

[226] A. Carpinteri and F. Mainardi(eds). Fractals and fractional calculus in continuum mechanics. *International Centre for Mechanical Sciences (Courses and Lectures), vol 378. Springer, Vienna*, pages 291–348, 1997.

[227] E. E. Adams and L. W. Gelhar. Field study of dispersion in a heterogeneous aquifer, 2 spatial moments analysis. *Water Resources Research*, 28(12):3293–3307, 1992.

[228] F. Mainardi. Fractional relaxation oscillation and fractional diffusion swave phenomena. *Chaos, Solitons and Fractals*, 7(9):1461–1477, 1996.

[229] M. Caputo. Diffusion of fluids in porous media with memory. *Geothermics*, 28(1):113–130, 1999.

[230] I. M. Sokolov, J. Klafter, and A. Blumen. Ballistic versus diffusive pair dispersion in the richardson regime. *Physical review E*, 61(3):2717, 2000.

[231] C. Yin, Y. Q. Chen, and S. Zhong. Fractional order sliding model based extremum seeking control of a class of nonlinear system. *Automatica*, 50(12):3173–3181, 2014.

[232] C. Li and G. Peng. Chaos in chen's system with a fractional order. *Chaos, Solitons and Fractals*, 22(2):443–450, 2004.

[233] R. Gorenflo, F. Mainardi, D. Moretti, and P. Paradisi. Time fractional diffusion: a discrete random walk approach. *Nonlinear Dynamics*, 29(1):129–143, 2002.

[234] C. F. M. Coinmbra. Mechanics with variable-order differential operators. *Annalen der physik*, 12(11–12):692–703, 2003.

[235] R. Metzler and J.Klafter. Boundary value problems for fractional diffusion equations. *Physica A: Statistical Mechanics and its Applications*, 278(1):107–125, 2000.

[236] R. Gorenflo, Y. Luchko, and F. Mainardi. Wright functions as scaleinvariant solutions of the diffusion wave equation. *Journal of Computational and Applied Mathematics*, 118(1):175–191, 2000.

[237] O. P. Agrawal. A general solution for the fourth-order fractional diffusion-wave equation. *Fractional Calculus and Applied Analysis*, 3(1):1–12, 2000.

[238] O. P. Agrawal. A general solution for a fourth order fractional diffusion wave equation defined in a bounded domain. *Computers and Structures*, 79(16):1497–1501, 2001.

[239] O. P. Agrawal. Response of a diffusion-wave system subjected to deterministic and stochastic fields. *ZAMM-Journal of Applied Mathematics and Mechanics*, 83(4):265–274, 2003.

[240] R. Metzler and J. Klafter. The random walk's guide to anomalous diffusion: a fractional dynamics approach. *Physics Reports*, 339(1):1–77, 2000.

[241] B. I. Henry and S. L. Wearne. Fractional reaction-diffusion. *Physica A: Statistical Mechanics and its Applications*, 276(3):448–455, 2000.

[242] T. Kosztolowicz. Subdiffusion in a system with a thick membrane. *Journal of Membrane Science*, 320(1):492–499, 2008.

[243] Y. Zhang, M. Meerschaert, and B. Baeumer. Particle tracking for time fractional diffusion. *Physical Review E*, 78(3):1–7, 2008.

[244] M. Dehghan, M. Abbaszadeh, and A. Mohebbi. Analysis of a meshless method for the time fractional diffusion wave equations. *Numerical algorithms*, 73(2):445–476, 2016.

[245] V. R. Hosseini, E. Shivanian, and W. Chen. Local radial point interpolation (MLRPI) method for solving time fractional diffusion-wave equation with damping. *Journal of Computational Physics*, 312:307–332, 2016.

[246] P. M. Jordan and A. Puri. Digital signal propagation in dispersive media. *Journal of Applied Physics*, 85(3):1273–1282, 1999.

[247] J. Banasiak and J. R. Mika. Singular perturbed telegraph equations with applications in the random walk theory. *Journal of Applied Mathematics and Stochastic Analysis*, 11(1):9–28, 1998.

[248] V. H. Weston and S. He. Wave splitting of the telegraph equation in r^3 and its application to inverse scattering. *Inverse Problems*, 9(6):789–812, 1993.

[249] A. Saadatmandi and M. Dehghan. Numerical solution of hyperbolic telegraph equation using the Chebyshev Tau method. *Numerical Methods for Partial Differential Equations*, 26(1):239–252, 2010.

[250] A. Saadatmandi and M. Mohabbati. Numerical solution of fractional telegraph equation via the Tau method. *Mathematical Reports*, 17(67):155–166, 2015.

[251] J. Chen, F. Liu, and V. Anh. Analytical solution for the time fractional telegraph equation by the method of separating variables. *Journal of Mathematical Analysis and Applications*, 338(2):1364–1377, 2008.

[252] L. Beghin and E. Orsingher. The telegraph process stopped at stable distributed times and its connection with the fractional telegraph equation. *Fractional Calculus and Applied Analysis*, 6(2):187–204, 2003.

[253] W. Jiang and Y. Lin. Representation of exact solution for the time fractional telegraph equation in the reproducing kernel space. *Communications in Nonlinear Science and Numerical Simulation*, 16(9):3639–3645, 2011.

[254] V. R. Hosseini, W. Chen, and Z. Avazzadeh. Numerical solution of fractional telegraph equation by using radial basis functions. *Engineering Analysis with Boundary Elements*, 38:31–39, 2014.

[255] J. Tang and D. Xu. The global behavior of finite difference spatial spectral collocation methods for a partial integro differential equation with a weakly singular kernel. *Numerical Mathematics: Theory, Methods and Applications*, 6(3):556–570, 2013.

[256] P. Camino. A numerical method for a PDE with memory. *Proceedings of the 9th CEDYA, Valladolid*, pages 107–112, 1987.

[257] M. E. Gurtin and A. C. Pipkin. A general theory of heat conduction with finite wave speed. *Archive for Rational Mechanics and Analysis*, 31(2):113–126, 1968.

[258] R. K. Miller. An integro differential equation for rigid heat conductors with memory. *Journal of Mathematical Analysis and Applications*, 66(2):313–332, 1978.

[259] T. Tang. A finite difference scheme for partial integro-differential equations with a weakly singular kernel. *Applied Numerical Mathematics*, 11(4):309–319, 1993.

[260] M. Renardy. Mathematical analysis of viscoelastic flows. *Annual review of fluid mechanics*, 21(1):21–34, 1989.

[261] C. Chen, V. Thomée, and L. B. Wahlbin. Finite element approximation of a parabolic integro differential equation with a weakly singular kernel. *Mathematics of computation*, 58(198):587–602, 1992.

[262] D. Xu. Finite element methods for the nonlinear integro-differential equations. *Applied mathematics and computation*, 58(2–3):241–273, 1993.

[263] L. Wulan and D. Xu. Finite central difference/finite element approximations for parabolic integro differential equations. *Computing*, 90(3):89–111, 2010.

[264] M. Dehghan. Solution of a partial integro-differential equation arising from viscoelasticity. *International Journal of Computer Mathematics*, 83(1):123–129, 2006.

[265] R. F. Warming and B. J. Hyett. The modified equation approach to the stability and accuracy analysis of finite difference methods. *Journal of Computational Physics*, 14(2):159–179, 1974.

[266] G. Fairweather. Spline collocation methods for a class of hyperbolic partial integro differential equations. *SIAM journal on numerical analysis*, 31(2):444–460, 1994.

[267] S. S. Siddiqi and S. Arshed. Cubic B-spline for the numerical solution of parabolic integro differential equation with a Weakly Singular Kernel. *Research Journal of Applied Sciences, Engineering and Technology*, 7(10):2065–2073, 2014.

[268] Y. Q. Huang. Time discretization scheme for an integro differential equation of parabolic type. *Journal of Computational Mathematics*, 12(3):259–263, 1994.